REQ. NO. 6-9015
CONTRACT REPORT NO. 69015-01-SQ

ACCRETION GROWTH AT THE TUYERES OF A PEIRCE-SMITH COPPER CONVERTER

by

A.A. Bustos
J.K. Brimacombe
G.G. Richards

The Centre for Metallurgical Process Engineering
The University of British Columbia
Vancouver, B.C. V6T 1W5

January 1987

Submitted to the Department of Supply & Services
Under the terms of Contract Number
23440-9015/01 ST

67pp

MICROMEDIA

ABSTRACT

In copper converting, accretions form at the tip of the tuyeres, and may block the air flow which then necessitates punching. In this study, observations have been made of accretions in a Peirce-Smith converter at the Inco Copper Cliff Smelter by viewing through the mouth when the vessel was rolled out of the stack. In addition, a mathematical model, based on heat and mass transfer, has been developed to predict the size and shape of accretions as a function of several variables: blast pressure, blast flow rate, oxygen enrichment, stage of the converting cycle, bath superheat and bath composition. Thus it has been found that accretion formation is most pronounced during the slagmaking stage, particularly toward its completion, and early in the coppermaking blow. Increasing the air flow rate or decreasing the bath superheat enhances accretion growth. With increasing oxygen enrichment of the blast, the size of the accretion diminishes until at about 36 pct. O_2, the tuyereline is virtually exposed. Raising the blast pressure to achieve choked (sonic) flow in the tuyeres increases the length of the accretion, but as has been shown previously, does not cause tuyere blockage. This again shows the advantage of high-pressure injection by virtue of protecting the tuyereline with accretions of a length sufficient to move the oxidizing gases farther from the refractory backwall. Finally, conditions conducive to tuyere blockage under normal low-pressure conditions have been studied by considering the solidification of a semi-infinite liquid during the time that bath washes against the tip of

the accretion between the discharge of successive gas bubbles. This again shows that blockage will be worst late in the slagmaking blow.

RÉSUMÉ

Durant le convertissage du cuivre, il se forme une agglomération au bout des tuyères ce qui peut bloquer l'entrée d'air, d'où la nécessité du poinçonnage. Dans cette étude, des observations ont été effectuées sur les agglomérations, dans un convertisseur Pierce Smith à l'Inco Copper Cliff Smelter en regardant à travers la bouche du convertisseur lorsque le four était tourné. De plus, un modèle mathématique basé sur le transfert de chaleur et de masse, a été développé dans le but de prédire la grosseur et la forme des agglomérations en fonction de plusieurs variables: pression de la poussée d'air, le débit d'air, l'enrichissement en oxygène, l'étape du cycle de convertissage, la température ainsi que la composition du bain. Ainsi, on a trouvé que la formation d'agglomérations est plus prononcée durant l'étape de la formation de scorie, plus particulièrement vers la fin de cette étape, et au début du soufflage lors de la formation du cuivre. Le fait d'accroître le débit d'air ou d'abaisser la température du bain, aggrave la formation des agglomérations. Avec l'enrichissement d'oxygène dans la poussée d'air la grosseur des agglomérations diminue. A 36% O_2 d'enrichissement, les bouts des tuyères sont presque complètement exposées. L'augmentation de la pression de la poussée d'air, pour obtenir un débit à la vitesse du son dans les tuyères, accroît la longueur des agglomérations, mais comme déjà démontré, ne cause pas le blocage des tuyères. Ceci démontre, encore une fois, l'avantage de l'injection à haute pression par rapport à la protection des tuyères avec des agglomérations de longueurs suffisantes permettant de déplacer les gaz oxydants loin des briques réfractoires. Finalement, les conditions incitant le blocage des tuyères lors des conditions normales à basse pression ont été étudiées en considérant la solidification d'un liquide semi-infini pendant que le bain liquide mouille le bout des agglomérations entre les échappements de bulles d'air successives. Ceci démontre que le blocage sera plus prononcé vers la fin du soufflage de l'étape de la formation de la scorie.

INTRODUCTION

The discharge of cold gas into a hot molten bath frequently leads to the freezing of accretions at the tuyere tip, depending on the local heat balance. In the Peirce-Smith converting process, accretions are a particular problem because at the low blowing pressures employed (< 100 kPag) they block the tuyeres and must be dislodged by mechanical or manual "punching" to restore the air flow. Under these conditions, the accretions are deleterious to the process because they adversely reduce the air flow rate; and perhaps more importantly, the required punching accelerates refractory wear at the tuyere line which limits the campaign life of the converter lining.

The adverse impact of accretion formation in the Peirce-Smith converter is in marked contrast to the exploitation of accretions in submerged injection steelmaking processes, such as AOD, which operate with much higher injection pressures. In the latter, injection conditions are established to solidify accretions around the tuyere tip for the purpose of locally protecting the refractory lining from high reaction temperatures without blocking the tuyeres. This can be accomplished provided that the injection pressure is sufficiently high to achieve sonic choked flow in the tuyeres. Brimacombe et al.[1-3] have shown that at these higher pressures, giving rise to sonic velocity in the tuyeres, the gas discharges as a continuous jet which prevents liquid from contacting the tuyere tip to form accretions that block the gas flow. At lower pressures, the gas issues discontinuously from the

tuyeres in the form of "bubbles" which facilitate the formation of accretions that cover the tuyere mouth and interfere with gas flow. Bustos et al.[4] have observed the growth of such accretions with the aid of a tuyerescope during blowing in Peirce-Smith copper converters. Both Brimacombe et al.[1-3] and Kimura et al.[5] have shown that the introduction of elevated pressure to achieve choked flow (Mach 1 in the tuyere) prevents tuyere blockage and the need to punch tuyeres.

Owing to the critical role accretions play in the converting process, it is important to assess the influence of factors which contribute to accretion formation under both conventional and high-pressure injection conditions in the Peirce-Smith converter. Although studies of accretion growth have been conducted for the steelmaking processes, as shall be seen, there are important differences to copper converting which consists of separate slagmaking and coppermaking stages. Thus simple extrapolation of results from the ferrous work is not fruitful. Questions concerning the effect of gas flow rate, oxygen enrichment and bath temperature on the formation of accretions in the different stages of converting are addressed in the present study. The disadvantage of low-pressure blowing will be seen since punchless or "free" blowing is only possible if accretion growth is suppressed with the consequence that refractory at the tuyere line is exposed to hot oxidizing conditions. The formation of accretions that protect the tuyere line refractory, but do not block tuyeres, is only possible under high-pressure, choked-flow conditions.

PREVIOUS WORK

The mechanism of accretion formation in both ferrous and non-ferrous gas injection processes has been investigated in the laboratory and mathematically. Boxall et al.[6] reported a simple experimental technique to simulate knurdle formation and growth by injecting cooled gas into a transparent liquid such as water. Xu et al.[7,8] also developed an aqueous model to study the formation of ice accretions by injecting supercooled helium into a bath of water. The accretion growth rate was found to be proportional to time, gas flow rate and gas "supercool" temperature, and inversely proportional to liquid "superheat" temperature.

Using the relaxation technique, Krivsky and Schuhmann[9] predicted the temperature distribution in the refractory wall surrounding the tuyere pipe in a copper converter. They indicated that the cooling effect of the gas flow in the tuyere was the cause of accretions. They also pointed out that the tuyere zone in a copper converter could be designed in such a way that tuyere punching would be unnecessary. Later, Pehlke[10] indicated that the solution of Krivsky and Schuhmann is influenced markedly by the grid spacing and that one of the major factors in the time and cost requirements on the computer is the accuracy of the initial refractory temperature distribution.

Boxall et al.[6] developed a mathematical model to predict the shape of knurdles in their physical model and to allow the relevance of the model studies to real injection processes to be assessed. Their mathematical model considered the heat-transfer process between the liquid in the tank and the injected gas. The model examined a steady-state situation after a knurdle had been formed, with its dimensions remaining constant as time passes; vertical conduction was neglected and the heat flux from the bath was assumed horizontal. Preliminary results showed agreement between both models.

Sahai and Guthrie[11] studied several factors governing the formation and growth of metallic mushrooms during shrouded-gas injection operations in steelmaking. They carried out a thermal analysis of the accretion growth, in which the heat removed by the protective gas equals the heat supplied by the hot metal and the heat released on solidification of the metal. They also considered the conditions toward the end of the blow, during which steady state is achieved, that is, no growth of the accretions. From this analysis it was concluded that a balance between heating and cooling factors was established, wherein approximately 60 percent of the maximum cooling capability of the shrouding hydrocarbon gas is available for freezing a protective accretion of steel around a tuyere.

Ohguchi and Robertson[12] carried out calculations to estimate the conditions under which pipe-shaped accretions form in steelmaking furnaces by considering heat transfer both in the refractory around the

tuyere and in the molten metal. They also developed a porous-accretion model for heat transfer and accretion formation around a tuyere in order to calculate shapes of mushroom-like accretions[13]. For the pipe-shaped accretions it was found that the thermal conductivity of the refractory affects the bottom radius of the accretions, but does not affect the height. Accretion height was a maximum at a particular value of the heat-transfer coefficient between accretion and gas. The accretion grows in the form of a narrow tube increasing in height and rapidly reaches its maximum value; thereafter the knurdle increases in radius to slowly reach its steady-state shape. During accretion growth, the temperature distribution in the refractory changes significantly due to the cooling caused by the gas flow. This leads to considerable thermal stresses in the refractory. For both types of accretion, a decrease in superheat or an increase of gas flow rate increase the size of the accretion.

SCOPE OF THE PRESENT STUDY

None of the previous investigations has addressed accretion growth at the tuyeres of a copper converter in either the coppermaking or slagmaking stages. Thus the major goal of this project was to study and to understand the effect of several factors that promote accretion formation at the tuyereline of Peirce-Smith converters. The objectives of the study can be summarised as follows:

(i) To analyse the phenomenon of accretion formation at the tuyeres of Peirce-Smith converters and to determine factors governing their shape and size.

(ii) To interpret results obtained from previous conventional- and high-pressure injection tests in Peirce-Smith converters.

(iii) To determine operating conditions under which the formation of accretions does not lead to tuyere blockage and prevents excessive erosion of the tuyereline refractory, i.e. optimum injection conditions (pressure and flow rate, tuyere diameter, oxygen enrichment of the blast, bath temperature).

The work has consisted of two parts. Firstly plant trials were conducted at the Noranda Horne Smelter and Inco Copper Cliff Smelter in which accretions at the tuyereline were photographed through the mouth of the converter after it was rolled out of the stack at different stages of the coppermaking cycle. In addition to conventional low-pressure blowing conditions, high-pressure injection was investigated. Secondly, a mathematical model of accretion growth was formulated, based on heat and mass transfer principles, to quantify the influence of process variables on the shape and size of the accretions.

PLANT TRIALS

The industrial trials have been described in detail by Bustos et al.[3]. At both the Horne and Copper Cliff Smelters it was found that

a minimum pressure of 276 kPag (40 psig) was necessary to prevent blockage of test tuyeres having diameters of 25-32 mm (1-1.25 in). This pressure is just sufficient to maintain sonic choked flow conditions in the tuyere as reported by Brimacombe et al.[1-2]. In these tests, observation of the accretions through the converter mouth revealed similarity between the high- and low-pressure tuyeres. In general, the accretion formation was found to depend on the stage of the converter cycle and the temperature of the bath. This could be seen from the blowing rate as well as from observation of accretions. Figure 1 shows the injection rate of air through a single 32-mm dia. tuyere operating at 276 kPag, together with the total air flow rate to the conventional tuyeres, during the blowing of Charge No. 2 (flash-furnace matte) at the Copper Cliff Smelter. As can be seen, an average flow rate of 18.4-19.8 Nm^3/min (650-700 scfm) was measured for the high-pressure tuyere. Toward the end of the slag blow (220-260 min. elapsed time in Figure 1) the flow rate through the high-pressure tuyere decreased by about 30 pct. to 14.2 Nm^3/min (500 scfm). Similarly, punching of the low-pressure tuyeres was necessary after 180 min. of blowing, and the overall air flow rate also drops toward the end of the slag blow. This reduction in the air flow rate was more pronounced whenever the bath was overoxidized.

Figures 2 and 3 show accretions, having a cylindrical shape, formed during the slagmaking blow of a flash-furnace matte charge at the Copper Cliff Smelter. Under normal conditions, i.e. no over blowing of the charge, a pipe-shaped accretion is formed with a diameter of about

60-80 mm, as indicated in Figure 2. However, at the end of the slagmaking blow, when the bath has been overoxidized, Figure 3, the diameter of the accretion is about 100-140 mm, much larger than in the previous situation. During the copper blow, the size of the accretions is significantly smaller. Reduction in flow rate through the high-pressure or conventional tuyeres (and punching of the latter) was observed when the bath temperature dropped due to the addition of cold material.

As suggested earlier, the pressure at which air is injected apparently does not alter the mechanism by which accretions are formed but its effect on tuyere blockage is important. Under conventional low-pressure conditions, a relatively minor build-up at the tuyere tip significantly reduces the air flow into the converter. At the Horne Smelter, accretions covering less than 50 pct. of the tuyere cross-sectional area, as observed through the back of a tuyere with a tuyere-scope, reduced the total flow rate from about 708 Nm^3/min (25,000 scfm) to less than 510 Nm^3/min (18,000 scfm). On the other hand, when the injection pressure was 276 kPag (40 psig) or higher, the tuyere flow rate was constant even though a substantial accretion build up was occurring at the tuyere tip.

The high-pressure injection technique has also been applied in a 6-ton Peirce-Smith pilot converter by Kimura et al.[5]. The results of these tests indicated that for sonic choked flow conditions there is no tuyere blockage and punching is not needed although accretions are

formed around the tip of the tuyeres. By controlling the shape of the accretions, the life of the refractory around the tuyere zone was reported to be three times longer than that under normal injection conditions. Oxygen enrichment of the blast above 40 pct. produced severe refractory erosion.

MODELLING OF THE ACCRETION FORMATION PROCESS

A schematic diagram of the accretion formation zone is presented in Figure 4 showing the cylindrical tuyere, the trajectory of the injected air in the bath and the refractory around the tuyere. All temperature gradients in the bath were assumed to be confined to a thermal diffusion zone adjacent to the accretion and refractory walls. The same concept was applied earlier by Ohguchi and Robertson[12]. The thickness of the thermal diffusion zone was determined by considering conduction across it to be equivalent to convective heat flow between the bath and the accretion.

Other major assumptions made to develop the model are the following:

(i) The jet of gas penetrating into the bath is continuous and has the same effective diameter as the tuyere.

(ii) The bulk liquid temperature is homogeneous due to strong agitation of the bath.

(iii) Axial symmetry.

(iv) Constant material properties of gas, refractory and metal.

(v) The system is at steady-state.

(vi) The instantaneous composition of the bath and the accretion are identical.

(vii) The instantaneous bath composition is homogeneous. No slag is considered.

The governing heat-transfer equation for the bath, the accretion and the refractory in a two-dimensional cylindrical system is:

$$\frac{\partial^2 T}{\partial z^2} + \frac{1}{r}\frac{\partial T}{\partial r} + \frac{\partial^2 T}{\partial r^2} = 0 \qquad (1)$$

The heat-balance equation for the blast flowing through the tuyere is:

$$Q_m C_p \frac{dT_B}{dz} = 2\pi r_o h_{B/T}[T_W - T_B] \qquad (2)$$

Similarly, the heat-balance equation for the blast flowing through the accretion is:

$$Q_m C_p \frac{dT_B}{dz} = 2\pi r_o h_{B/A}[T_W - T_B] \qquad (3)$$

The boundary conditions for the different regions are as follows:

i) Outside surface of refractory

$$T = \text{constant} \tag{4}$$

ii) Interface between accretion and refractory

$$[k_m \frac{\partial T}{\partial z}]_A = [k_R \frac{\partial T}{\partial z}]_R \tag{5}$$

$$[T]_A = [T]_R \tag{6}$$

iii) Interface between thermal diffusion zone and refractory

$$[k_m \frac{\partial T}{\partial z}]_M = [k_R \frac{\partial T}{\partial z}]_R \tag{7}$$

$$[T]_d = [T]_R \tag{8}$$

iv) Interface between accretion and thermal diffusion zone

$$[k_m \frac{\partial T}{\partial z}]_A = [k_m (\frac{\partial T}{\partial z})]_d \tag{9}$$

$$[T]_A = [T]_d = T_{m.p.} \tag{10}$$

v) Interface between bulk liquid and fictitious thermal diffusion zone

$$[T]_d = T_{bath} \tag{11}$$

vi) Interface between accretion and gas

$$h_{B/A}[T_W - T_B] = k_m \frac{\partial T}{\partial r}\Big|_{r = r_o} \tag{12}$$

vii) Tuyere/blast interface

$$h_{B/T}[T_W - T_B] = k_R \frac{\partial T}{\partial r}\Big|_{r = r_o} \tag{13}$$

viii) External boundary of the cylindrical region (no net heat flow)

$$\frac{\partial T}{\partial r}\Big|_{r = r_{max}} = 0 \tag{14}$$

ix) Interface between bath and injected air (tip of the accretion). At the tip of the accretion, heat is generated due to the exothermic oxidation reactions. The rate of heat generation can be characterized in terms of the oxygen mass-transport rate and the enthalpy of the reactions. Ashman et al.[14] have shown that the overall slagmaking reaction:

$$FeS + 1.5\ O_2 = FeO + SO_2 \tag{15}$$

and the blister-making reaction

$$Cu_2S + O_2 = 2Cu + SO_2 \qquad (16)$$

are both controlled by the rate of oxygen transport within the gas phase, which can be described by

$$n_{O_2} = k_{O_2} A_{int} \frac{P^b_{O_2}}{RT_{int}} \qquad (17)$$

Therefore the heat generation due to the exothermic reactions taking place at the tip of the accretion is

$$H_{B/A} = \Delta H_R \, n_{O_2} = \Delta H_R \, k_{O_2} \, A_{int} \, P^b_{O_2}/RT_{int} \qquad (18)$$

where ΔH_R is the heat of reaction (per mole of O_2) of the respective oxidation reactions. In the calculation, this reaction heat was treated as a local heat source at the blast/melt boundary and was conducted into the accretion and thermal diffusion zone.

Equation (1) was solved with the blast heat-balance equations and boundary conditions by the successive relaxation or Gauss-Seidel point-by-point method[9,15,16] in which the values of the variables are calculated by visiting each grid point in a certain order. To start this systematic trial-and-error method, a linear temperature profile was assumed for each point in the grid. Then point-by-point calculations were made repeatedly through each element, continually adjusting the

point temperatures, until the final set of point temperatures satisfied the basic heat-flow equations. The trial calculation at each point consisted of calculating the net heat flow to that point from the surrounding points. Under steady state conditions the net heat flow to a given point should be zero. After the first calculation of the net heat flow, the temperatures of the points were replaced by the calculated values. The convergence of this iterative approach was guaranteed by the fact that the finite-difference equations satisfied the Scarborough criterion for convergence[16]. The finite-difference mesh employed for the calculations is shown in Figure 5. The total number of mesh points was 528. Small mesh intervals in the vicinity of the gas conduit and close to the refractory-melt interface were chosen.

The actual computation was done on an Eagle Plus-2 P.C. and a typical run consumed about 150 minutes of computer time.

Data and Numerical Constants

Values for the material properties at injection conditions are shown in Tables 1 and 2. The thermal conductivity of the refractory, 1.4 $W\ m^{-1}{}_{\circ}C^{-1}$,[21] is that of a typical chrome-magnesite brick. Unfortunately the thermal conductivities of copper mattes were not available from the literature and therefore an estimate of their values was necessary. To this end the empirical expression suggested by Smith

and Palmer[17,18] to calculate the thermal conductivity of copper alloys was employed. The Smith and Palmer equation predicts the thermal conductivity of the melt, k_m, from known values of k_e, the electrical conductivity:

$$k_m = L\, k_e\, T + a \qquad (19)$$

where: $L = 2.38 \times (10^{-8})\, W\, °C^{-2}\, ohm$

and $a = 75.06\, W\, m^{-1}\, °C^{-1}$

Table 3 shows the calculated values of the thermal conductivities of mattes with different copper contents.

The heat-transfer coefficient between the blast and the tuyere pipe was calculated by means of the Colburn analogy[15,25] for fluids having Prandtl numbers in the range 0.5 to 100 under turbulent flow conditions

$$Nu = 0.023\, Re^{0.8}\, Pr^{1/3} \qquad (20)$$

Values of the heat-transfer coefficient for the blast air in the tuyere pipe region under various blowing rates and tuyere diameters under fully developed conditions (long pipes) are presented in Table 4.

The blast heat-transfer coefficient in the accretion zone was calculated assuming that the internal diameter of the accretion is the same as the diameter of the tuyere and that the roughness of the internal surface of the accretion is much larger than that of the tuyere pipe. Under these conditions, and using the results of Nunner[26,19] for air injection into rough tubes, the value of the blast/accretion heat-transfer coefficient is approximately two times larger than the blast/tuyere heat-transfer coefficient calculated from Eq.(20).

To take into account the effect of the abrupt contraction entrance at the back of the tuyere, the expressions proposed by McAdams[27] were employed to modify the value of the heat-transfer coefficients previously described

$$h_{entrance} = h[1 + (\frac{d_o}{\ell})^{0.7}], \quad 2 < \frac{\ell}{d_o} < 20 \tag{21}$$

and

$$h_{entrance} = h[1 + 6\,\frac{d_o}{\ell}], \quad \frac{\ell}{d_o} > 20 \tag{22}$$

where ℓ is the distance from the back of the tuyere body.

The heat-transfer coefficient between the molten bath and the accretion, used to determine the thickness of the thermal diffusion zone, was calculated from the correlation for heat transfer of liquid metals in cross flow over a tube bank[15]

$$Nu = 4.03 + 0.228\ (RePr)^{0.67} \qquad (23)$$

or

$$Nu = 4.03 + 0.228\ \left(\frac{vd\rho C_p}{k_m}\right)^{0.67} \qquad (24)$$

In this case, v, the velocity of the bath close to the accretion was assumed to be 0.25 ms^{-1}, from measurements in a 100 ton converter operating at a blast volume of 640 m^3/min[28]. This value also agrees well with bath circulation velocities calculated by Ashman et al.[14] for bubble frequencies of the order of 4 s^{-1}. The external diameter of the accretion was considered to be 80 mm for this calculation. Table 5 shows values of the heat-transfer coefficient between the bath and the accretion for various thermal conductivities. The physical properties of the Cu_2S-Cu mixtures were assumed to be a linear function of their composition.

The oxygen mass-transfer coefficient at the tip of the accretion (or at the tip of the tuyere if no accretion is formed) was calculated by means of the correlation for a wetted-wall column[29]:

$$Sh = 0.023\ Re^{0.83}\ Sc^{0.33} \qquad (25)$$

which is analogous to the correlation for heat transfer to fluids flowing turbulently inside tubes. Table 6 shows values of the oxygen mass-transfer coefficient under different injection conditions.

The heats of reaction during slagmaking and coppermaking blows were calculated assuming a bath temperature of 1200°C and the blast air at 25°C. Tables 7 and 8 show the corresponding heat balances for each case.

Typical blowing parameters studied under low-pressure and high-pressure injection conditions are summarized in Table 9.

RESULTS

Results for accretion formation under low-pressure injection conditions are presented in Figure 6, which shows the shape of the accretion, isotherms in the refractory and temperature of the blast flowing through the tuyere region and the accretion zone. The bath conditions correspond to the slagmaking part of the blow with 75% Cu matte. The change in the air temperature is not significant in the tuyere but is noticeable in the accretion due to the high heat-transfer coefficient and the large thermal conductivity of the solidified matte.

The effect of bath temperature on accretion formation with low-pressure injection into the same 75% Cu matte is shown in Figure 7. The accretion length is considerably affected by bath superheat becoming greater than 300 mm for a superheat of less than 100°C. The bottom radius of the accretion is less sensitive to variations in bath temperature.

The influence of blast flow rate on accretion formation and temperature of the air flowing through the tuyere and accretion can be

observed in Figures 8 and 9, respectively. For the relatively low tuyere flow rate of 0.24 kg s^{-1} (420 scfm) the length and average thickness of the accretion are about 230 and 6 mm, respectively. On the other hand, for an injection flow rate of 0.36 kg s^{-1} (635 scfm) the length of the accretion formed increases to 300 mm and its average thickness to about 10 mm.

As the converting of matte proceeds, the composition of the bath and consequently its thermal conductivity changes. From Equation (24) it is clear that changes in the conductivity of the matte also modify the heat-transfer coefficient between the accretion and the melt, the bath circulation velocity assumed to be constant. Figure 10 shows the effect of bath thermal conductivity on accretion formation under low-pressure injection conditions. An increase in the thermal conductivity (and the bath/accretion heat-transfer coefficient) increases the heat transferred from the surrounding liquid and the accretion becomes shorter and thinner. It is important to note that for these calculations the melting point of the matte was assumed to be constant (1130°C); this is not a realistic assumption because changes in the bath composition also imply variations of its melting point.

The effect of bath composition on accretion formation for a bath superheat of 110°C can be seen in Figure 11. For these calculations, changes in the thermal conductivity and melting point of the bath were taken into account. At the beginning of the slagmaking

blow (matte 50% Cu, Figure 11a) the length of the accretion is 170 mm and its average thickness about 8 mm. As the converting process proceeds, the size of the accretion increases such that close to the end of slagmaking (matte 75% Cu, Figure 11b), its length is 280 mm. The accretion thickness, however, remains unchanged. During the coppermaking blow, the oxidation of white metal generates much less heat per mole of oxygen than the slagmaking reaction (Tables 7 and 8). As a consequence, during the early stages of blister copper production (white metal 90% Cu_2S-10% Cu, Figure 11c) the length of the accretion increases to 340 mm. As the coppermaking stage continues, there is a continuous increase in the thermal conductivity of the bath and the length of the accretion is reduced to 280 and 20 mm for bath compositions of 80% Cu_2S-20% Cu (Figure 11d) and 50% Cu_2S-50% (Figure 11e), respectively. Close to the end of the coppermaking stage the increase in thermal conductivity of the bath is such that there is no accretion build-up at the tip of the tuyere.

Figure 12 compares the accretion formation process under low-pressure and high-pressure injection conditions. The calculations were carried out for three different air flow rates which are typical of normal converting practice. A tuyere back pressure of 103 kPag and tuyere diameter of 50 mm were used for this case. In order to obtain similar flow rates for a tuyere diameter of 32 mm, the tuyere back pressure has to be of the order of 275 kPag. As can be observed in Figure 12, high-pressure injection produces longer and thicker accretions

as compared with its low-pressure counterpart. For an air flow rate of 0.30 kg s^{-1}, the predicted length of the low-pressure accretion is about 280 mm and its average thickness about 8 mm, whereas under high-pressure conditions, the length and thickness of the accretion are 380 mm and 12 mm, respectively. As in the case of low-pressure injection, for high-pressure injection, an increase in air flow rate increases the length and thickness of the accretion.

As can be observed from Eq.(24), changes in the bath circulation velocity close to the accretion region affect the heat-transfer coefficient between the bath and the accretion. The effect of the latter variable on accretion formation under high-pressure injection conditions is presented in Figure 13. Under standard conditions, i.e. bath circulation velocity about 0.25 ms^{-1} ($h_{m/A}$ = 9820 $Wm^{-1}{}^{\circ}C^{-1}$) the accretion length and average thickness are 380 and 10 mm respectively. If the bath circulation velocity is raised, the length and thickness of the accretion decrease as the heat transfer from the liquid to the solidified bath increases. For a bath velocity of about 0.35 ms^{-1} ($h_{m/A}$ = 12200 W $m^{-2}{}^{\circ}C^{-1}$) the length of the accretion is 340 mm and its average thickness less than 8 mm.

If the oxygen level in the blast air increases, the rate of oxygen transport to the air/bath interface (Eq.(17)) increases, and as a consequence, the heat generated due to the oxidation reactions taking

place at the tip of the accretion increases. The effect on the size of the accretion is shown in Figure 14. When air is injected through the tuyere, the length and average thickness of the accretion are 260 and 10 mm, respectively. As the oxygen enrichment level is increased to 28 pct. the accretion length is reduced to 150 mm and its thickness to about 8 mm. For an enrichment level of 32 pct. the length and thickness of the accretion are 70 and 6 mm respectively. Further increases in the oxygen level cause corresponding reductions in accretion size until at 36 pct. enrichment, the length of the accretion is less than 10 mm.

The effect of the stage of the blow on accretion formation is indicated in Figure 15. For these calculations a constant bath temperature of 1240°C was assumed throughout the cycle. Consequently the bath superheat changed as the blow proceeded. As mentioned earlier, during the converting process, the bath composition changes and, as a consequence, the thermal conductivity and the melting point of the bath also vary. At the beginning of the slag blow, the melting point of the matte (approximately 50% Cu) is relatively low, 1000°C, and its thermal conductivity (calculated according to the relationship of Smith and Palmer[17]) is 9.4 W $m^{-1}{}^{\circ}C^{-1}$. The length and thickness of the accretion formed at this stage of the blow are 70 and 2 mm, respectively. As the slagmaking stage proceeds, the thermal conductivity of the matte decreases and its melting point increases, so that close to the end of this part of the cycle (matte at approximately 75% Cu), they are 8.7 W $m^{-1}{}^{\circ}C^{-1}$ and 1130°C respectively. Under these conditions, the build-up

is severe; the length of the accretion is now 280 mm and its average thickness 8 to 10 mm. At the beginning of the coppermaking blow (white metal, 90% Cu_2S-10% Cu), the thermal conductivity of the bath is 21.2 W $m^{-1}{}^{\circ}C^{-1}$, its melting point 1125°C and the heat generation at the tip of the accretion is 1.75×10^5 J per mole O_2 as compared to 2.97×10^5 J per mole O_2 during the slagmaking stage. The combined effect of all these factors tends to produce accretions that are longer (320 mm) and thinner (7 mm) than those generated close to the end of slagmaking. As the coppermaking stage continues, there is a substantial increase in the thermal conductivity of the melt while its melting point decreases. As a consequence the accretions being formed become shorter as the blow proceeds. As indicated in Figure 15, for a white metal composition of 80% Cu_2S-20% Cu (thermal conductivity 33.7 W $m^{-1}{}^{\circ}C$, melting point 1120°C) the length of the accretion is about 250 mm and its average thickness is 6 mm, whereas for a white metal composition of 50% Cu_2S-50% Cu, the accretion is virtually non-existent.

DISCUSSION

Validity of the Model

The predictions of the mathematical heat-transfer model developed to calculate accretion formation agree well with observations of operating Peirce-Smith copper converters. A comparison of Figure 2 with results from the model, say, Figure 11 or Figure 15, indicates that

both the shape and the size of the accretions predicted by the model are similar to the shapes and sizes found during actual converting practice. The model also indicates that the accretion formation process is more severe at the end of the slagmaking and beginning of the coppermaking blow; therefore blowing under normal low-pressure conditions will be more difficult during these stages owing to tuyere blockage accompanying the heavy build-up. Again this is a prediction confirmed by industrial observations, as Figure 1 indicates.

A major limitation of the present work has been the paucity of information available on thermophysical properties of copper mattes. Thus the effect of the composition of the matte (or the white metal) on thermal conductivity had to be estimated from expressions developed for copper alloys[17] and therefore their applicability to the present situation is limited. For the same reason, melting points, specific heats and densities for different compositions of matte and white metal had to be estimated by means of linear interpolations of values from the literature[22,23]. Also, owing to this lack of information, it was not possible to simulate the effect of different levels of magnetite in the matte realistically, and this task was not attempted.

Accretion Formation and Refractory Protection

As mentioned earlier, in steelmaking processes, the presence of accretions is beneficial because they protect the refractory surrounding

the tuyeres from excessive erosion. The control of accretion formation for this purpose is relatively straightforward in steelmaking because the thermophysical properties of the melt do not change as extensively as in the case of Peirce-Smith converting. Moreover, owing to the high injection pressure usually employed in these processes, the growth of accretions does not lead to tuyere blockage.

The refractory temperature in contact with the accretion changes markedly during the converting cycle. As can be seen in Table 10, assuming a constant bath superheat of 110°C, the temperature of the refractory/accretion interface closest to the tuyere increases from 563°C at the beginning of the slagmaking blow to 1030°C half-way through the coppermaking blow while the accretion diameter decreases by 11 mm. Thus as the converting cycle proceeds, the area surrounding the tuyere is less protected by accretions and is more susceptible to erosion of the refractory.

Accretion Formation and Tuyere Blockage

As was mentioned before, a major cause of refractory wear is the practice of punching tuyeres to prevent blockage. In the accretion formation model, the assumption that the jet of gas penetrating into the liquid melt has the same effective diameter as the diameter of the tuyere prevents the simulation of tuyere blockage. Nevertheless, from the results of the model it is possible to determine whether tuyere blockage would occur or not under a given set of low-pressure injection conditions.

Under normal, low-pressure conditions, air discharges into the converter in the form of bubbles. Between the release of one bubble and the formation of the next, bath washes for short periods against the tip of the tuyere (or the accretion). During these short periods it is possible that some solidification of bath takes place on the inside of the tuyere (or accretion) wall, depending on the stage of the converting cycle, bath superheat and temperature of the wall. If this solidification process is continued repeatedly, it will block the tuyere after a certain period.

In order to predict conditions under which tuyere blockage would occur, one can apply the analytical solution developed for the progress of solidification of a semi-infinite liquid phase. In the converter, the short-time event of bubble formation/bubble release is mathematically equivalent to a semi-infinite condition. If one assumes that at $t > 0$, the liquid initially at temperature, T_{bath}, is contacted with the accretion internal wall at temperature, T_{wall}, the liquid may solidify depending on local conditions; and the solidification front, $Y(t)$ will advance with time as follows:

$$Y(t) = 2\lambda \sqrt{\alpha_s t} \qquad (26)$$

The parameter λ is an unknown constant of proportionality, which for the situation under study can be evaluated by means of Equation (27) derived following the method of Carslaw and Jaeger[21] for the case where the bath and accretion have the same thermal conductivity and thermal diffusivity:

$$\frac{T_{bath} - T_{m.p}}{\lambda \exp(\lambda^2)\mathrm{erfc}(\lambda)} - \frac{T_{m.p} - T_{wall}}{\lambda \exp(\lambda^2)\mathrm{erfc}(\lambda)} = -\frac{\pi^{1/2} \Delta H_f}{C_{p,m}} \qquad (27)$$

When λ is positive, liquid will solidify on the accretion (and block it eventually after numerous bubbling events) whereas if λ is negative, the accretion in contact with the liquid will melt.

Table 11 presents results of calculations made for two sets of conditions, namely a constant bath temperature of 1240°C and a constant bath superheat of 110°C. As can be observed from the results, for a constant bath temperature of 1240°C, tuyere blockage would occur ($\lambda > 0$) only at the end of the slagmaking stage. For the case of a constant bath superheat of 110°C, tuyere blockage would occur throughout the entire slagmaking stage of the converting cycle, but would not take place during coppermaking. The advance of the solidification front (or tuyere blockage) is nevertheless relatively slow ($\lambda = 0.20$) during the early stages of the slagmaking cycle, as compared with the tuyere blockage ($\lambda = 1.24$) which occur at the end of this stage. These results agree well with industrial practice, in which tuyere blockage is more problematical late in the slagmaking cycle. The results also suggest that the pronounced blockage found during this part of the blow may not be the result of magnetite precipitation, as previously believed, but a direct result of the thermal conditions in the tuyere region at that particular moment.

Accretion Formation and High-Pressure Injection

The results of the model indicate that for an equivalent tuyere flow rate, the accretions formed under high-pressure injection are longer than their low-pressure counterparts; and therefore the oxidation reaction takes place farther away from the refractory backwall. This effect coupled with the fact that high-pressure tuyeres do not block so that punching is not necessary, explains the three-fold increase in refractory life reported by Kimura et al.[5].

In addition, during high-pressure injection, the oxygen mass-transfer coefficient is much larger than for low-pressure injection (Eq.(25) and Table 6). This suggests that the overall oxygen utilization of the process may be greater when a relatively small tuyere diameter and high-injection pressure are employed in the converter, although this would also depend on bubble break-up and local convection close to the tuyeres.

Accretion Formation and Oxygen Enrichment

The results of the model indicate that an oxygen enrichment level of the blast of about 36 pct. is the maximum level compatible with the formation of a protective layer of solidified material around the periphery of the tuyere refractory. Again these results agree with

industrial experience which indicates a maximum oxygen enrichment level in the range mentioned above. The results of the model also help to explain the severe refractory erosion reported by Kimura et al.[5] when 40 pct. oxygen enrichment was employed.

CONCLUSIONS

Accretion formation in the Peirce-Smith converter was studied in a series of in-plant trials and by the development of a mathematical model. The model satisfactorily predicts several characteristics of the converting process, under both low-pressure and high-pressure injection conditions. The results can be summarized as follows:

1. The accretions are almost cylindrical in shape, with a bottom radius of about 80 mm in most cases.
2. The accretion size changes significantly throughout the converting cycle. Early in the slagmaking stage the accretions are relatively short and as the cycle proceeds, they grow in length such that a maximum is reached at the end of the slagmaking/early coppermaking stages of the cycle. Thereafter there is a reduction in the accretion size such that by the middle of the coppermaking stage no accretions are formed. These predictions are in accord with the industrial observations. Decrease of superheat or increase of gas flow rate increases the size of the accretions.

3. Under high-pressure injection the accretions are longer than for a similar flow rate under normal, low-pressure conditions. Therefore for the former case the core of the converting reaction is farther away from the refractory than for low-pressure injection conditions. This effect, coupled with the fact that high-pressure tuyeres do not require punching, should significantly increase tuyereline refractory life.
4. The results of the model indicate that accretion formation takes place only up to an oxygen enrichment level of about 36 pct. Thereafter the tuyereline is unprotected, which is detrimental to refractory life.
5. A semi-quantitative analysis, based on the solidification of a semi-infinite liquid, was attempted to predict conditions under which tuyere blockage would occur. The results indicate that for a bath superheat of 110°C, tuyere blockage takes place throughout the entire slagmaking cycle. If the bath temperature is maintained at 1240°C, tuyere blockage would occur only toward the end of the slagmaking cycle but not during the early stages of slagmaking nor during the coppermaking stage of the blow.

ACKNOWLEDGEMENTS

The authors are most grateful to Inco, Noranda and CANMET (through DSS) for financial support of this study. We are particularly appreciative of the excellent cooperation received during the research and thank Noranda Research for providing a work place for A.A. Bustos.

LIST OF SYMBOLS

A_{int}	area of the gas/liquid melt interface, m^2
a	constant in Equation (19), W/m °C
C_p	specific heat, J/kg °C
$C_{p,m}$	specific heat of bath, J/kg °C
d	diameter of the accretion, m
d_o	diameter of the tuyere, m
H_T°	enthalpy at temperature, J
h	heat-transfer coefficient, W/m^2 °C
$h_{B/T}$	heat-transfer coefficient between tuyere and blast, W/m^2 °C
$h_{B/A}$	heat-transfer coefficient between accretion and blast, W/m^2 °C
$h_{m/A}$	heat-transfer coefficient between accretion and liquid melt, W/m^2 °C
$H_{B/A}$	heat generated at the blast/accretion interface, J/s
k_m	thermal conductivity of the melt and accretion, W/m °C
k_R	thermal conductivity of the refractory, W/m °C
k_{O_2}	oxygen mass transfer coefficient, m/s
k_e	electrical conductivity, $ohm^{-1}\ m^{-1}$
L	constant in Equation (19)
ℓ	distance from back of tuyere body, m
n_{O_2}	rate of oxygen transport in the gas phase, moles/s
Nu	Nusselt number
$P^b_{O_2}$	partial pressure of oxygen in the gas phase, atm
Pr	Prandlt number
Q_m	mass flow rate of injected gas, kg/s
r	radius, m
r_o	radius of tuyere, m

R	gas constant
Re	Reynolds number
Sc	Schmidt number
Sh	Sherwood number
t	time, s
T	temperature, °C
T_{bath}	temperature of the bulk liquid bath, °C
T_B	temperature of the blast, °C
T_d	temperature of the thermal diffusion zone, °C
T_{int}	temperature of the gas/liquid melt interface, K
T_W	temperature of the internal wall of the accretion, °C
$T_{m.p.}$	melting point of the bath, °C
$[T]_A$	temperature of accretion at interface with refractory or thermal diffusion zone, °C
$[T]_d$	temperature of thermal diffusion zone at interface with accretion, °C
$[T]_R$	temperature of refractory at interface with accretion or thermal diffusion zone, °C
v	bath circulation velocity, m/s
Y(t)	position of the solidification front, m
z	height, m
ΔH_f	heat of fusion (accretion), J
ΔH_R	heat of reaction for the slagmaking (or blistermaking) reactions, J/mole O_2
α_s	thermal diffusivity of the accretion and melt, m^2/s
δ	thickness of thermal diffusion zone, m
λ	constant of proportionality defined by Equation (26)
ρ	density of melt, kg/m^3

REFERENCES

1. E.O. Hoefele and J.K. Brimacombe, Metall. Trans. B 10B, 631 (1979).
2. J.K. Brimacombe, S.E. Meredith and R.G. Lee, Metall. Trans. B 15B, 243 (1984).
3. A.A. Bustos, J.K. Brimacombe, G.G. Richards, A. Vahed and A. Pelletier, To be presented at International Conference Copper 87, Viña del Mar, Chile, November 1987.
4. A.A. Bustos, G.G. Richards, N.B. Gray and J.K. Brimacombe, Metall. Trans. B 15B, 77 (1984).
5. T. Kimura, S. Tsuyuguchi, Y. Ojima, Y. Mori and Y. Ishii, J. of Metals 38(9), 38 (1986).
6. G. Boxall, A.K. Subharwal, T. Robertson and R.J. Hawkins, in Injection Phenomena in Extraction and Refining, A.E. Wraith, ed., University of Newcastle-upon-Tyne, 1982, pp. B1-B18.
7. C. Xu, Y. Sahai and R.I.L. Guthrie, in Injection Phenomena in Extraction and Refining, A.E. Wraith, ed., University of Newcastle-upon-Tyne, 1982, pp. K1-K27.
8. C. Xu, Y. Sahai and R.I.L. Guthrie, Ironmaking and Steelmaking 11(2), 101 (1984).
9. W.A. Krivsky and R. Schuhmann, Jr., Trans. TMS-AIME 215, 82 (1959).
10. R. Pehlke, Unit Processes of Extractive Metallurgy, Elsevier, New York, 1973.
11. Y. Sahai and R.I.L. Guthrie, Iron and Steelmaker 11(4), 34 (1984).

12. S. Ohguchi and D.G.C. Robertson, in Injection Phenomena in Extraction and Refining, A.E. Wraith, ed., University of Newcastle-upon-Tyne, 1982, pp. J1-J37.

13. S. Ohguchi and D.G.C. Robertson: Ironmaking and Steelmaking, 10(1), 15 (1983).

14. D.W. Ashman, J.W. McKelliget and J.K. Brimacombe, Can. Met. Quart. 20(4), 387 (1981).

15. F. Kreith, Principles of Heat Transfer, 3rd. Ed., Harper and Row, Publ., New York, 1973.

16. S.V. Patankar: Numerical Heat Transfer and Fluid Flow, Hemisphere Pub. Co., 1980.

17. C.S.A. Smith and E.W. Palmer, Trans. AIME, 117, 225 (1935).

18. M. Jakob, Heat Transfer, 2 Vols., John Wiley and Sons, 1949.

19. G.H. Geiger and D.R. Poirier, Transport Phenomena in Metallurgy, Addison-Wesley Publ. Co., 1973.

20. National Bureau of Standards, Circular 564, Tables of Thermal Properties of Gases, U.S. Government Printing Office, November 1955.

21. H.S. Carslaw and J.C. Jaeger, Conduction of Heat in Solids, 2nd Ed., Clarendon Press, Oxford, 1959.

22. A.K. Biswas and W.G. Davenport, Extractive Metallurgy of Copper, 2nd ed., Pergamon Press, 1980.

23. O. Kubaschewsky and C.B. Alcock, Metallurgical Thermochemistry, 5th ed., Pergamon Press, 1979.

24. G.M. Pound, G. Derge and G. Osuch, Trans. AIME 137, 481 (1955).

25. A.P. Colburn, Trans. AIChE 29, 1974 (1933).

26. W. Nunner, VDI-Forschungsheft No. 455, VDI Verlag GMBM, 1956.

27. W.M. McAdams, Heat Transmission, 3rd ed., McGraw-Hill Book Co., New York, 1954.

28. A.V. Spesivtsev, O. Ya. Galushko, V.P. Revin and L.S. Al'terman, Tsvetn. Met. (3), 3 (1978).

29. R.E. Treybal, Mass Transfer Operations, McGraw-Hill Book Co., New York, 1955.

LIST OF TABLES

Table 1. Physical Properties of Air and Oxygen at 300°C.

Table 2. Physical Properties of Various Bath Materials.

Table 3. Thermal Conductivities of Mattes.

Table 4. Blast/Tuyere Pipe Heat Transfer Coefficient ($h_{B/T}$).

Table 5. Melt/Accretion Heat Transfer Coefficient ($h_{m/A}$)

Table 6. Oxygen Mass Transfer Coefficient (k_{O_2}).

Table 7. Heat of Reaction During Slag Blow.

Table 8. Heat of Reaction During Copper Blow.

Table 9. Standard Injection Conditions.

Table 10. Temperature of the Tuyere at the Refractory/Accretion Interface ($T_{bath} - T_{m.p.} = 110°C$).

Table 11. Conditions for Tuyere Blockage.

TABLE 1

Physical Properties of Air and Oxygen at 330°C[19,20]

	AIR	OXYGEN
Density, kg m^{-3}	0.618	0.743
Specific heat, J kg^{-1} $°C^{-1}$	1044.2	-
Viscosity, kg $m^{-1}s^{-1}$	2.92×10^{-5}	3.30×10^{-5}
Thermal conductivity, W m^{-1} $°C^{-1}$	4.48×10^{-2}	-
Diffusivity (in air) m^2 s^{-1}	-	7.01×10^{-5}
Prandtl number	0.680	-
Schmidt number	-	0.634

TABLE 2

Physical Properties of Various Bath Materials

Material	Liquid Density at 1200°C (22) kg m^{-3}	Viscosity at 1200°C (22) kg $m^{-1}s^{-1}$	Melting Point (22) °C	Specific Heat at 1200°C (23) J kg^{-1} $°C^{-1}$
Matte 30% Cu	4100	1.0×10^{-2}	1050	726.8*
Matte 50% Cu	4600	1.0×10^{-2}	1000	671.7*
White Metal	5200	1.0×10^{-2}	1130	589.1*
Cu_2S	5200	-	1130	534.0
Blister Copper	7800	3.3×10^{-3}	1080	493.8

* Estimated value

TABLE 3

Thermal Conductivities of Mattes*

Material	Electrical Conductivity $ohm^{-1}\ cm^{-1}$ (22,24)	Thermal Conductivity $W\ m^{-1}\ °C^{-1}$
Matte 30% Cu	930	10.8*
Matte 50% Cu	520	9.4*
Matte 75% Cu	320	8.7*
Cu_2S	60	7.7*
Cu	5.85×10^5	133.9

* Calculated according to Equation (19)

TABLE 4

Blast/Tuyere Pipe Heat Transfer Coefficient ($h_{B/T}$)

	d_o = 32 mm		d_o = 50 mm	
Q_m, kg s^{-1}	Nu	$h_{B/T}$, $Wm^{-2}°C^{-1}$	Nu	$h_{B/T}$, $Wm^{-2}°C^{-1}$
0.239	520.1	728.8	364.0	325.6
0.299	622.2	870.4	435.4	390.4
0.359	720.2	1008.0	504.0	451.5

TABLE 5

Melt/Accretion Heat Transfer Coefficient ($h_{m/A}$)

k_m W $m^{-1}°C^{-1}$	Nu	$h_{m/A}$ W m^{-2} °C-1	Observations
5.0	129.0	8.07×10^3	
8.7	90.3	9.82×10^3	Matte 75% Cu_2S
9.4	85.9	1.02×10^4	Matte 50% Cu_2S
15.0	63.9	1.20×10^4	
21.2	49.8	1.32×10^4	90% Cu_2S + 10% Cu
30.0	41.6	1.56×10^4	
33.7	38.5	1.62×10^4	80% Cu_2S + 10% Cu
50.0	30.8	1.93×10^4	
71.3	26.4	2.35×10^4	50% Cu_2S + 50% Cu
133.9	20.1	3.37×10^4	Blister Copper

TABLE 6

Oxygen Mass Transfer Coefficient (k_{O_2})

Air Flow Rate		d_o = 50 mm		d_o = 32 mm	
$Nm^3\ s^{-1}$	$kg\ s^{-1}$	Sh	k_{O_2} $m\ s^{-1}$	Sh	k_{O_2} $m\ s^{-1}$
0.20	0.239	355.0	0.50	508.6	1.11
0.25	0.299	425.7	0.60	607.3	1.33
0.30	0.359	492.3	0.69	703.4	1.54

TABLE 7

Heat of Reaction During Slag Blow

$2/3\ FeS\ (1200°C) + O_2\ (25°C) \rightarrow 2/3\ FeO\ (1200°C) + 2/3\ SO_2\ (1200°C)$

Species	Heat Term	kJ
$2/3\ FeS_{(\ell)}$	$H°_{298} - H°_{1473}$	-73.1
O_2	$H°_{298} - H°_{298}$	0
$2/3\ FeS + O_2 = 2/3\ FeO + 2/3\ SO_2$	$\Delta H°_{298}$	-307.4
$2/3\ FeO$	$H°_{1473} - H°_{298}$	43.5
$2/3\ SO_2$	$H°_{1473} - H°_{298}$	40.5
Net Heat per mole O_2		-296.6

TABLE 8

Heat of Reaction During Copper Blow

Cu_2S (1200°C) + O_2 (25°C) $\rightleftarrows$ 2Cu (1200°C) + SO_2 (1200°C)

Species	Heat Term	kJ
$Cu_2S_{(\ell)}$	$H^\circ_{298} - H^\circ_{1473}$	-112.1
O_2	$H^\circ_{298} - H^\circ_{298}$	0
$Cu_2S + O_2 = 2Cu + SO_2$	ΔH°_{298}	-215.1
2Cu	$H^\circ_{1473} - H^\circ_{298}$	92.0
SO_2	$H^\circ_{1473} - H^\circ_{298}$	60.7
Net heat per mole O_2		-174.5

TABLE 9

Standard Injection Conditions

	Low-Pressure Injection	High-Pressure Injection
Tuyere diameter, mm (inch)	50 (2)	32 (1.25)
Injection pressure, kPag (psig)	103 (15)	275 (40)
Tuyere gas flow rate, $kg.s^{-1}$ (scfm)	0.299 (530)	0.299 (530)
Refractory thickness, m (inch)	0.3 (12)	0.3 (12)
Blast temperature, °C	50	50
Blast/Tuyere heat transfer coefficient, $W\ m^{-2}{}^{\circ}C^{-1}$	390.4	870.4
Blast/Accretion heat transfer, coefficient, $W\ m^{-2}{}^{\circ}C^{-1}$	780.8	1740.8
Melt/Accretion heat transfer coefficient, $W\ m^{-2}{}^{\circ}C^{-1}$	9820	9820
Oxygen mass transfer coefficient, $m\ s^{-1}$	0.6	1.33
Oxygen enrichment of the blast, pct. O_2	21	21
Heat of reaction during slag blow, J mole O_2^{-1}	297,000	297,000
Heat of reaction during copper blow, J mole O_2^{-1}	175,000	175,000
Bath circulation velocity, $m\ s^{-1}$	0.25	0.25

TABLE 10

Temperature of the Tuyere at the Refractory/Accretion Interface

$(T_{bath} - T_{m.p.} = 110°C)$

Material	$T_{m.p.}$ °C	T_{bath} °C	$T_{refractory/accretion}$ °C	Accretion Bottom Diameter, mm
Matte, 50%Cu	1000	1110	563	78
Matte, 75%Cu	1130	1240	576	83
White Metal 90%Cu_2S-10%Cu	1125	1235	781	83
White Metal 80%Cu_2S-20%Cu	1120	1230	882	80
White Metal 50%Cu_2S-50%Cu	1105	1215	1030	67

TABLE 11

Conditions for Tuyere Blockage

				T_{bath} = 1240°C		$T_{bath}-T_{m.p.}$=110°C	
MATERIAL	$T_{m.p.}$ °C	C_p $Jkg^{-1}°C^{-1}$	ΔH_f Jkg^{-1}	T_{wall} °C	λ	T_{wall} °C	λ
Matte, 50%Cu	1000	671.5	$1.8x10^5$	904	-0.23	813	+0.20
Matte, 75%Cu	1130	589.1	$8.7x10^4$	900	+1.24	900	+1.24
90%Cu_2S-10%Cu	1125	530.0	$8.2x10^4$	1027	-0.025	1025	-0.035
80%Cu_2S-20%Cu	1120	526.0	$9.6x10^4$	1069	-0.175	1062	-0.14
50%Cu_2S-50%Cu	1105	513.9	$1.4x10^5$	1089	-0.195	1090	-0.16

LIST OF FIGURE CAPTIONS

Figure 1. Operating conditions during a flash-furnace matte charge at Inco Copper Cliff Smelter. Numbers at top of figure refer to successive slag blows.

Figure 2. Pipe-shaped accretion during slagmaking blow of a flash-furnace matte charge at Inco Copper Cliff Smelter.

Figure 3. Accretion growth during over blowing of a flash furnace matte charge at Inco Copper Cliff Smelter. End of slagmaking.

Figure 4. Schematic of the accretion formation zone. Numbers refer to boundary condition equations in the text.

Figure 5. Finite-difference mesh for the heat transfer calculations.

Figure 6. Accretion formation under low pressure injection.

Figure 7. Effect of bath temperature on accretion formation.

Figure 8. Effect of blast flow rate on accretion formation.

Figure 9. Effect of blast flow rate on air temperature.

Figure 10. Effect of thermal conductivity of the bath on accretion formation.

Figure 11. Effect of bath composition on accretion formation.

Figure 12. Accretion formation under low-pressure and high-pressure injection conditions.

Figure 13. Effect of bath/accretion heat-transfer coefficient under high-pressure injection conditions.

Figure 14. Effect of oxygen enrichment on accretion growth. Low-pressure injection.

Figure 15. Effect of stage of the blow on accretion formation.

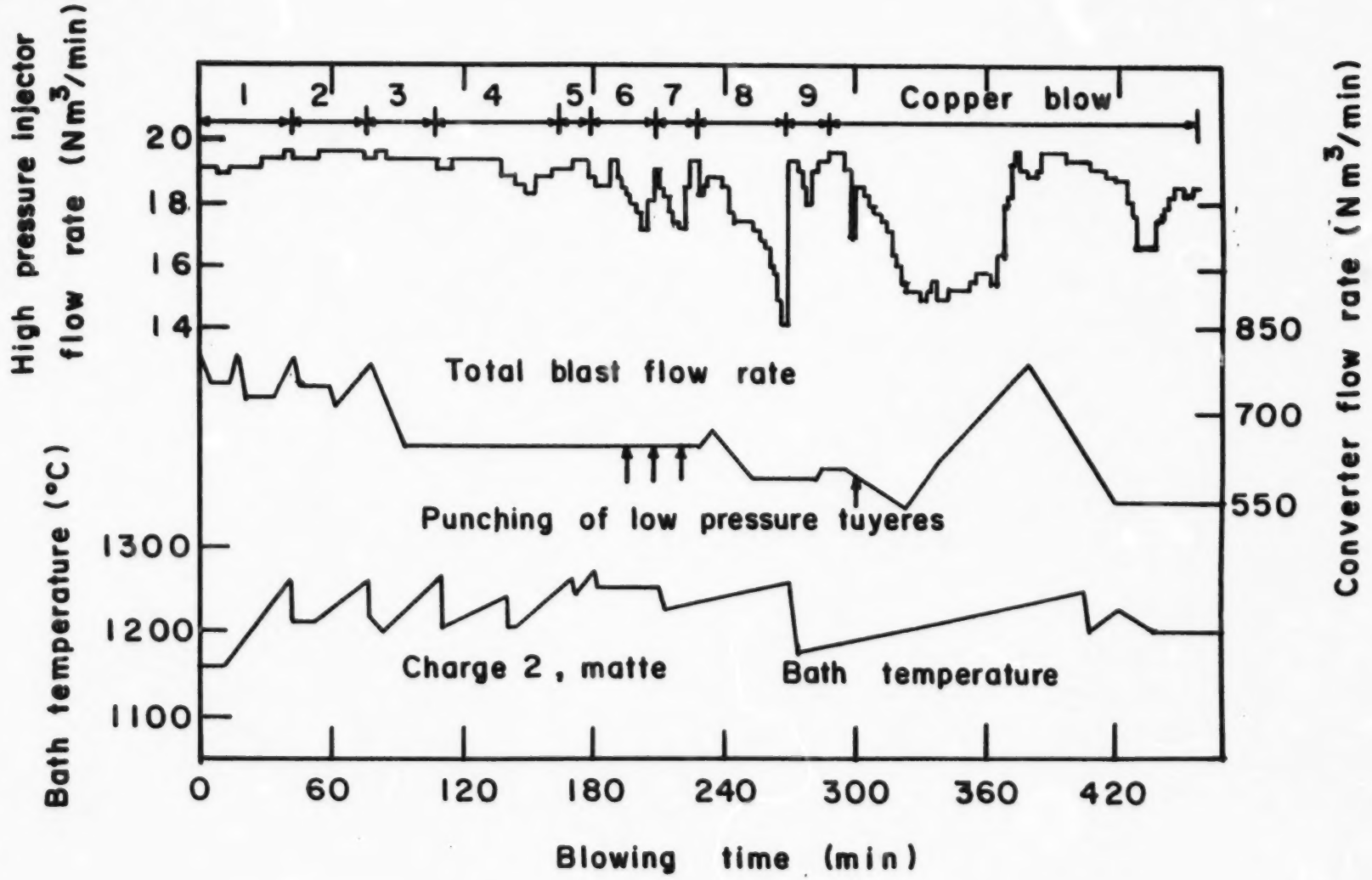

Figure 1. Operating conditions during a flash-furnace matte charge at Inco Copper Cliff Smelter. Numbers at top of figure refer to successive slag blows.

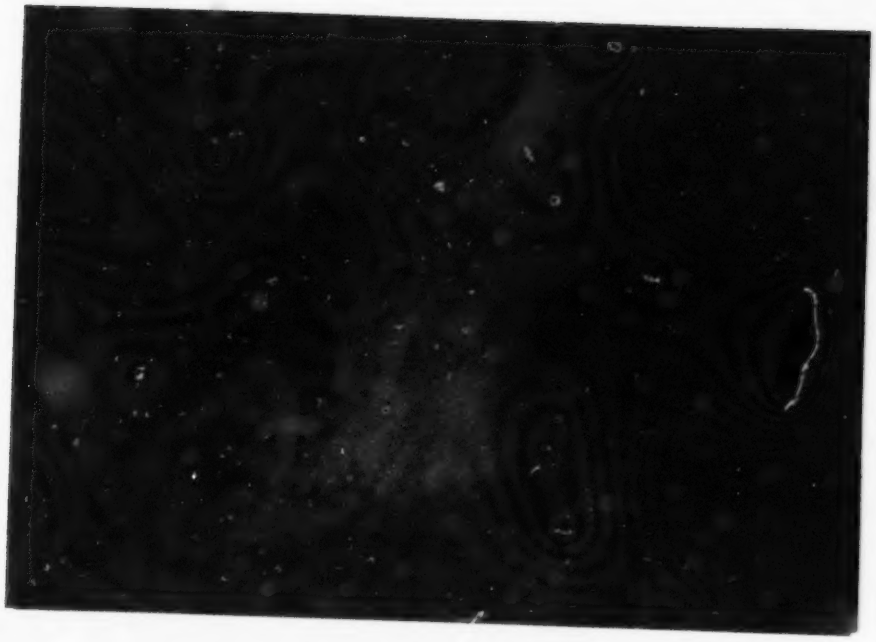

Figure 2. Pipe-shaped accretion during slagmaking blow of a flash-furnace matte charge at Inco Copper Cliff Smelter.

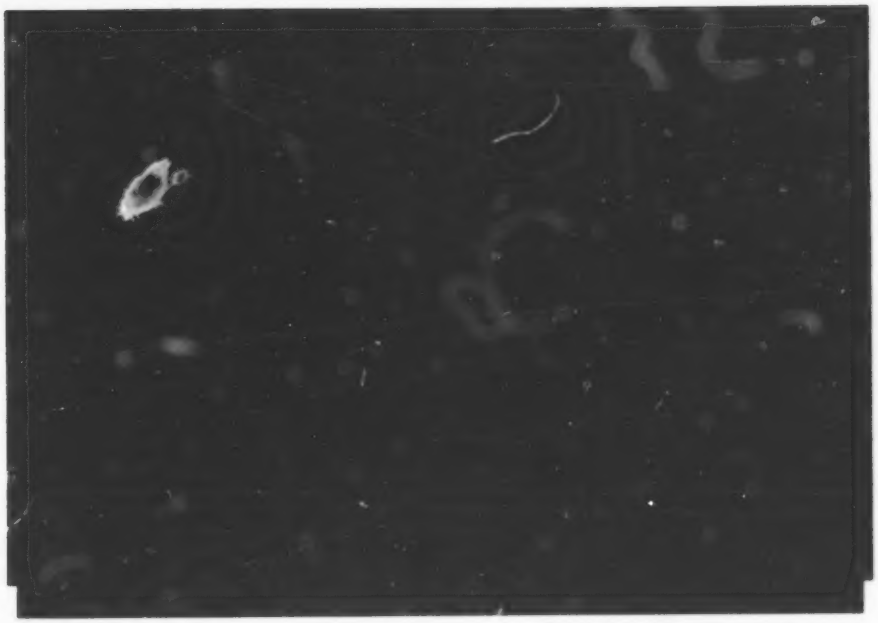

Figure 3. Accretion growth during over blowing of a flash furnace matte charge at Inco Copper Cliff Smelter. End of slagmaking.

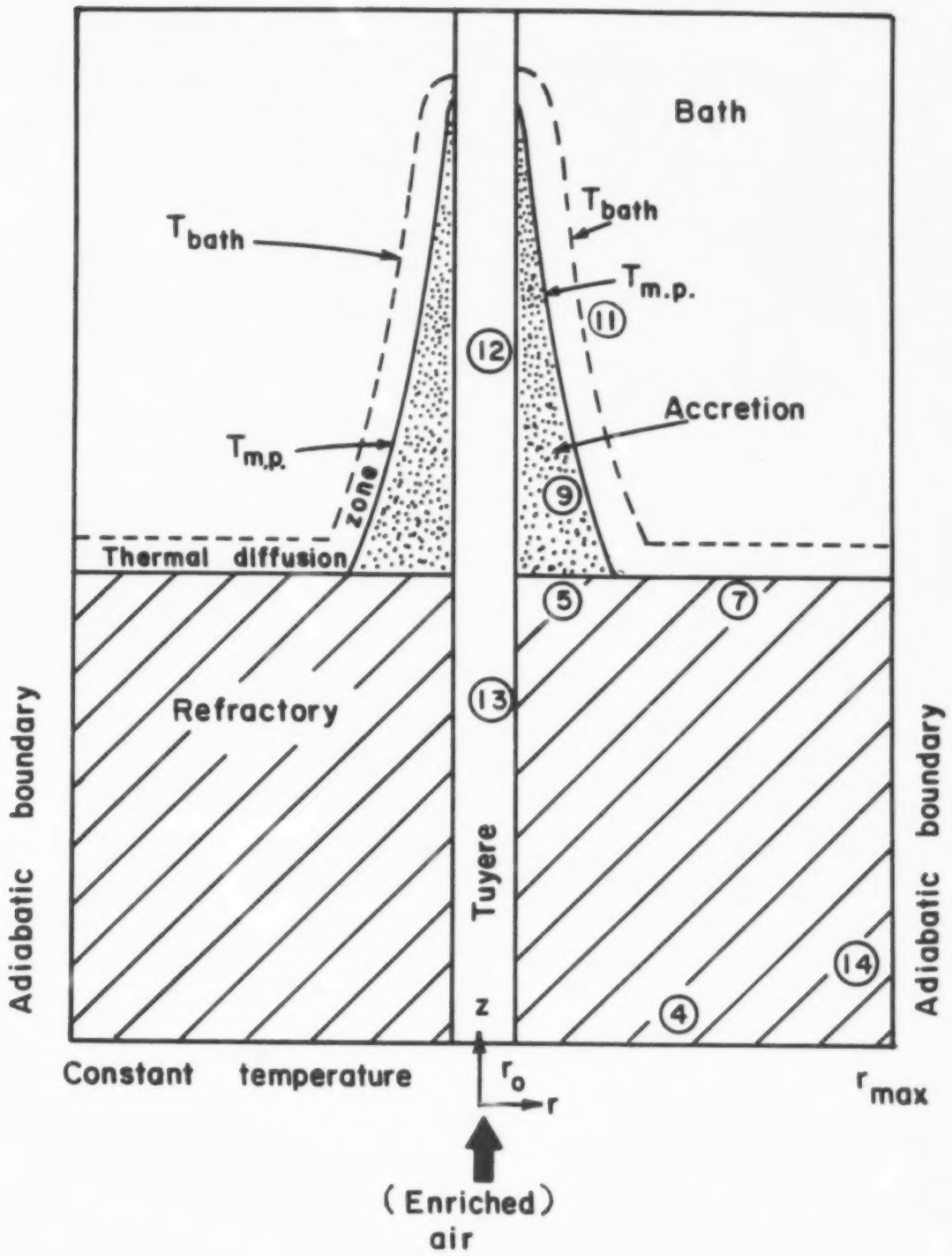

Figure 4. Schematic of the accretion formation zone.

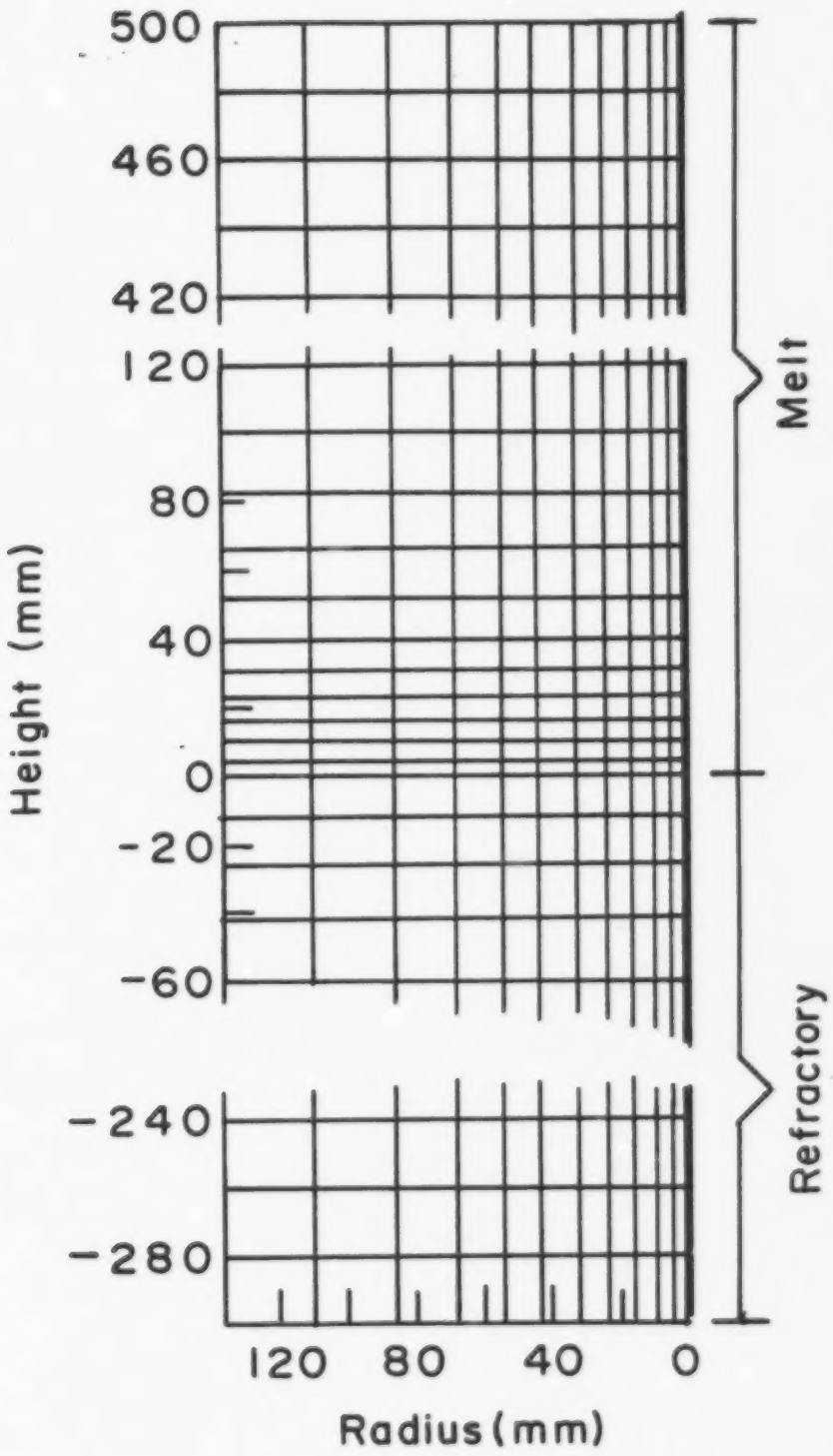

Figure 5. Finite-difference mesh for the heat transfer calculations.

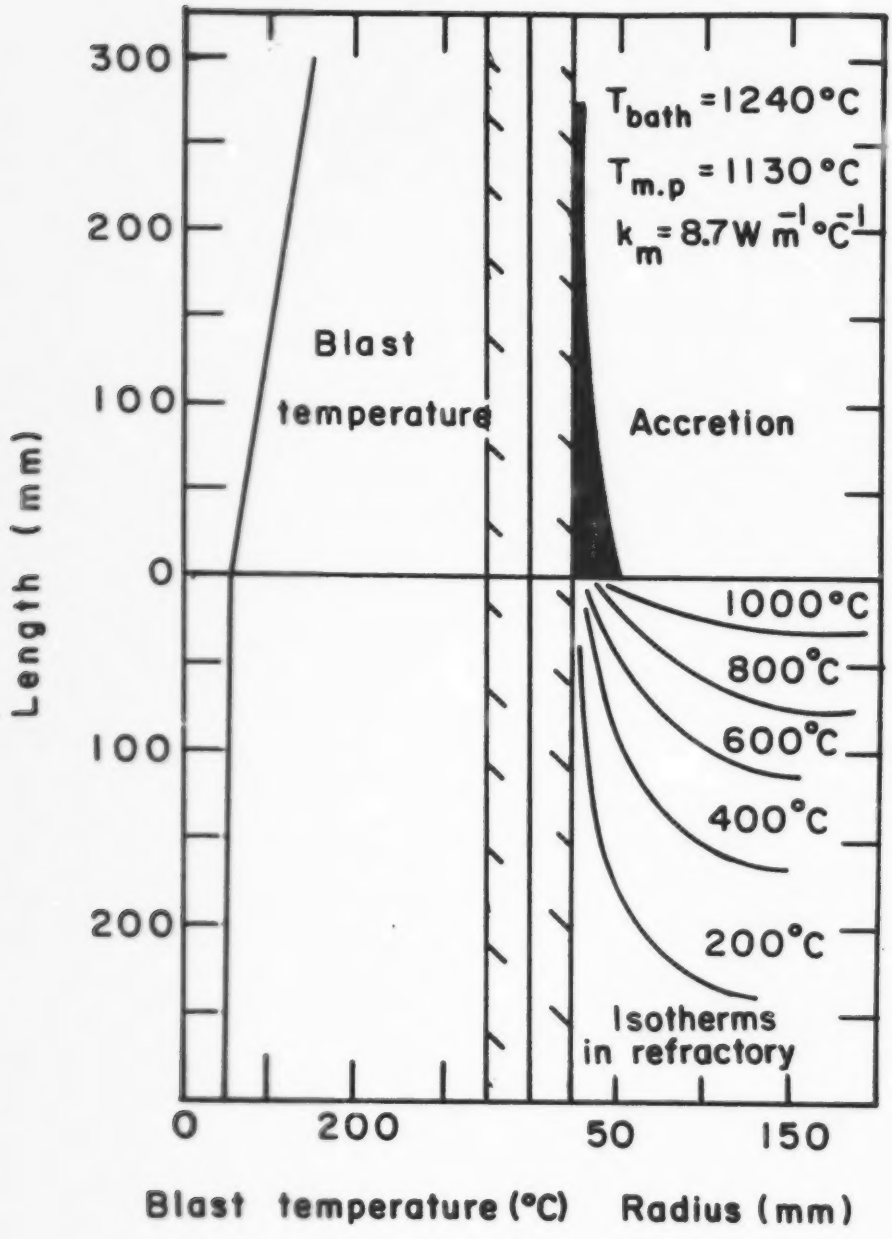

Figure 6. Accretion formation under low-pressure injection.

CANMET
MAY 5 1987
NOT CIRCULATION

CANMET
CONTRACT SUMMARY SHEET
AS AT April 14, 1987
FISCAL YEAR 86/87

TITLE: PUNCHLESS OPERATION OF PEIRCE SMITH CONVERTERS. PHASE II - ECONOMIC EVALUATION

CONTRACTOR: UNIVERSITY OF BRITISH COLUMBIA

SCIENTIFIC AUTHORITY: BELL DH

TEL: 6139964981

BEGIN/END: 9-May-1986 - 15-Nov-1986

REQUISITION NUMBER: 6-9015-

FUNDING

CANMET:	$0.00
CONTRACTOR:	$0.00
SSC:	$0.00
OTHER:	0.00
TOTAL:	$0.00

PROGRAM: MINERALS R & D

ACTIVITY: MINERAL PROCESSING

SUB-ACTIVITY: MINERAL PROCESSING

SUB-SUB-ACTIVITY: EXTRACTION - METALLIC

PROJECT: IMPURITIES IN COPPER REFINING

OBJECTIVES

In the Pierce-Smith copper converter accretions form at the tip of the tuyere during the blowing operation. In conventional practice, using low-pressure air (<100 kPag), the accretions block the tuyeres and must be dislodged by "punching" to restore the flow of air. The accretions are deleterious to the process because they substantially reduce the flow of air and the required punching causes wear and deterioration of the refractory at the tuyere-line, thus limiting the campaign life of the refractory lining of the converter. In a previous study (Contract #23440-4-9259) it was shown that blowing with high-pressure air (>276 kPag) prevented the blockage

.../2

PROCEDURE

A mathematical model of accretion growth, based on heat and mass transfer principles was developed, to quantify the influence of process variables on the shape and size of accretions. The process variables considered were: blast pressure, blast flow rate, oxygen enrichment, stage of the converting cycle, bath super heat and bath composition.

RESULTS

It has been found that accretion formation is most pronounced during the slagmaking stage, particularly toward its completion, and early in the coppermaking blow. Increasing the air flow rate or decreasing the bath superheat enhances accretion growth. With increasing oxygen enrichment of the blast, the size of the accretion diminishes until at about 36 pct. O_2, the tuyere-line is virtually exposed. Raising the blast pressure to achieve choked (sonic) flow in the tuyeres increases the length of the accretion, but as has been shown previously, does not cause tuyere blockage. This again shows the advantage of high-pressure injection by virtue of protecting the tuyere-line with accretions of a length sufficient to move the oxidizing gases farther from

.../2

APPLICATION AND ONGOING WORK

A copper producer is considering plans to convert one converter to high-pressure air. The test will determine the productivity gains provided by the use of high-pressure air due to the greater flow-rate of air available, and to the expected increase in campaign life of the infractory lining.

SUPPORTING DOCUMENTS

OBJECTIVES (Cont'd.)

of test tuyeres having diameters 25-32 mm. and eliminated the need to punch the tuyeres. The objectives of the present study are:

1) To analyse the phenomenon of accretion formation at the tuyeres of Pierce-Smith converters and to determine factors governing their size and shape.

2) To interpret results obtained from previous conventional and high-pressure air injection tests in P-S converters.

3) To determine operating conditions under which the formation of accretions does not lead to tuyere blockage and prevents excessive erosion of the tuyere-line refractory, i.e. optimum injection conditions (pressure, flow rate, tuyere diameter, oxygen enrichment of the blast and bath temperature).

RESULTS (Cont'd.)

the refractory backwall. Finally, conditions conducive to tuyere blockage under normal low-pressure conditions have been studied by considering the solidification of a semi-infinite liquid during the time that the bath washes against the tip of the accretion between the discharge of successive gas bubbles. This again shows that blockage will be worst late in the slagmaking blow.

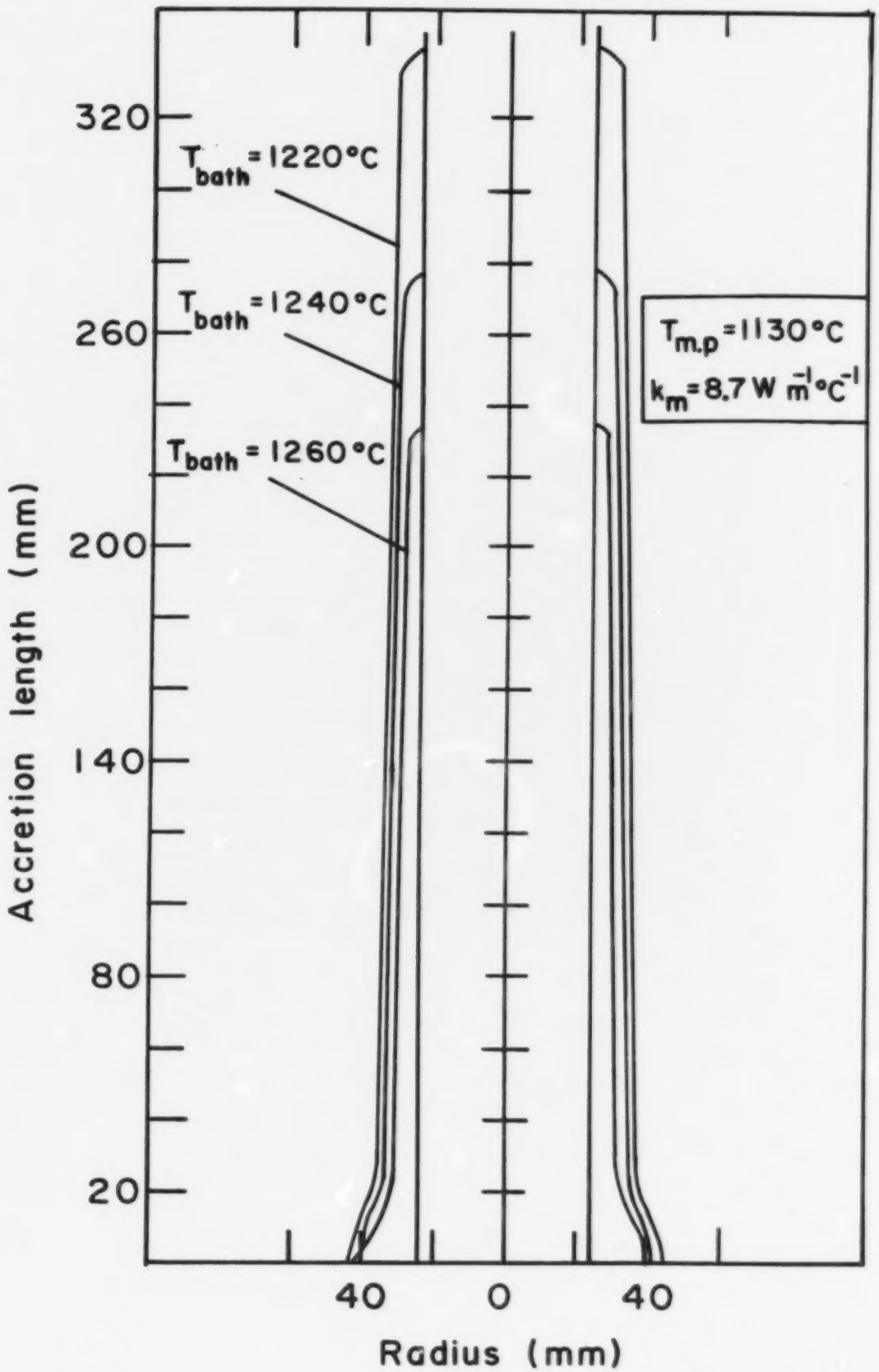

Figure 7. Effect of bath temperature on accretion formation.

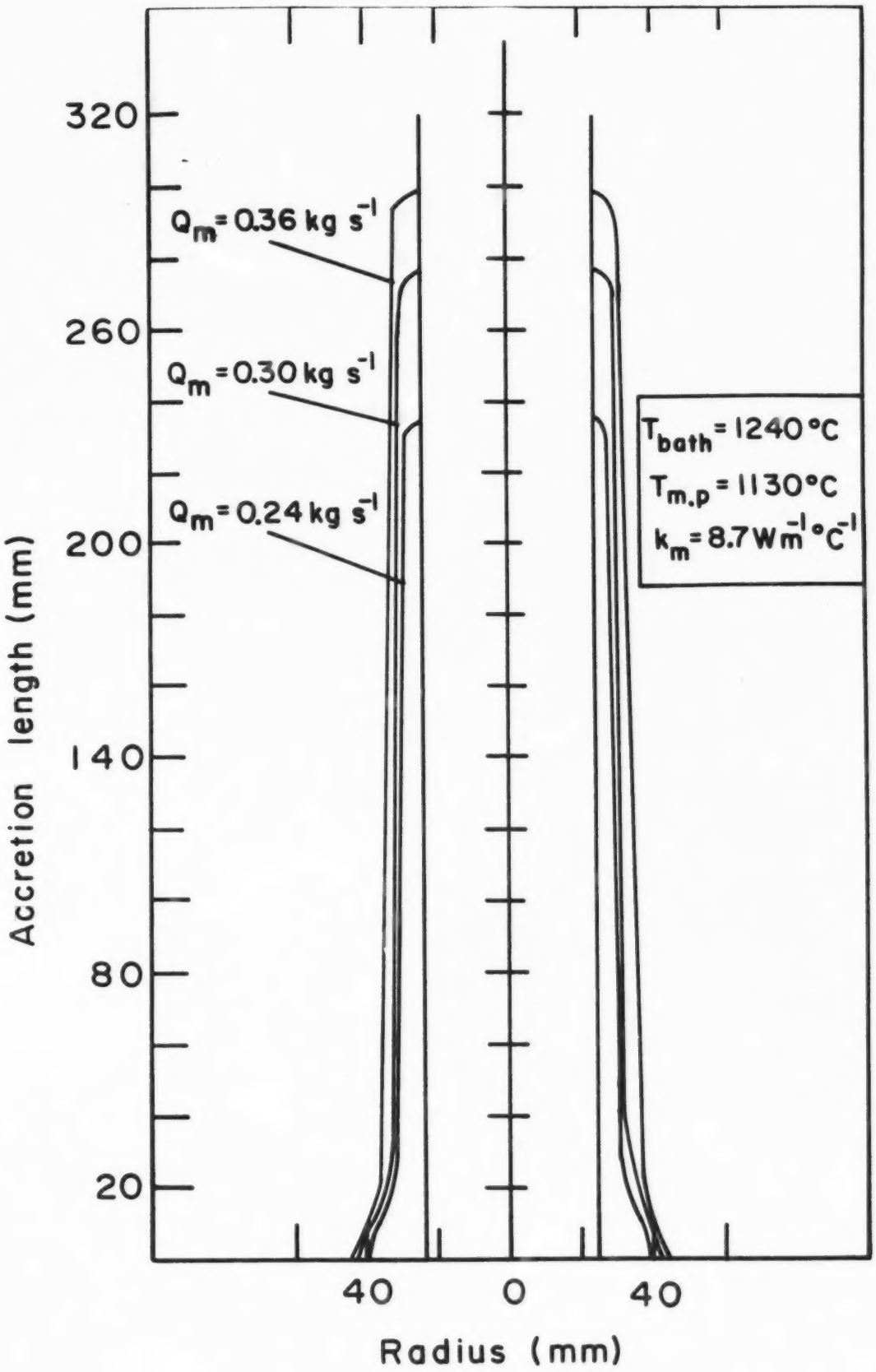

Figure 8. Effect of blast flow rate on accretion formation.

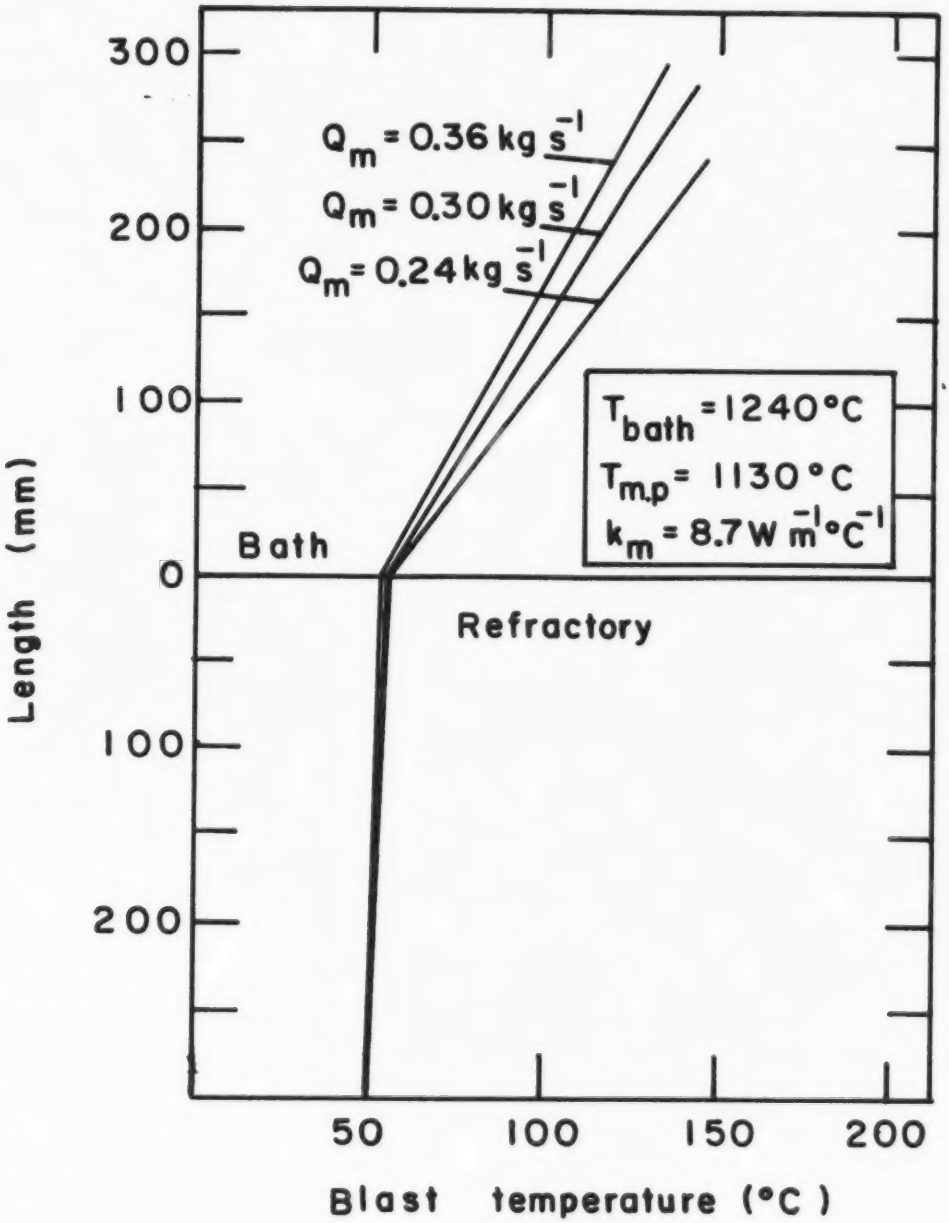

Figure 9. Effect of blast flow rate on air temperature.

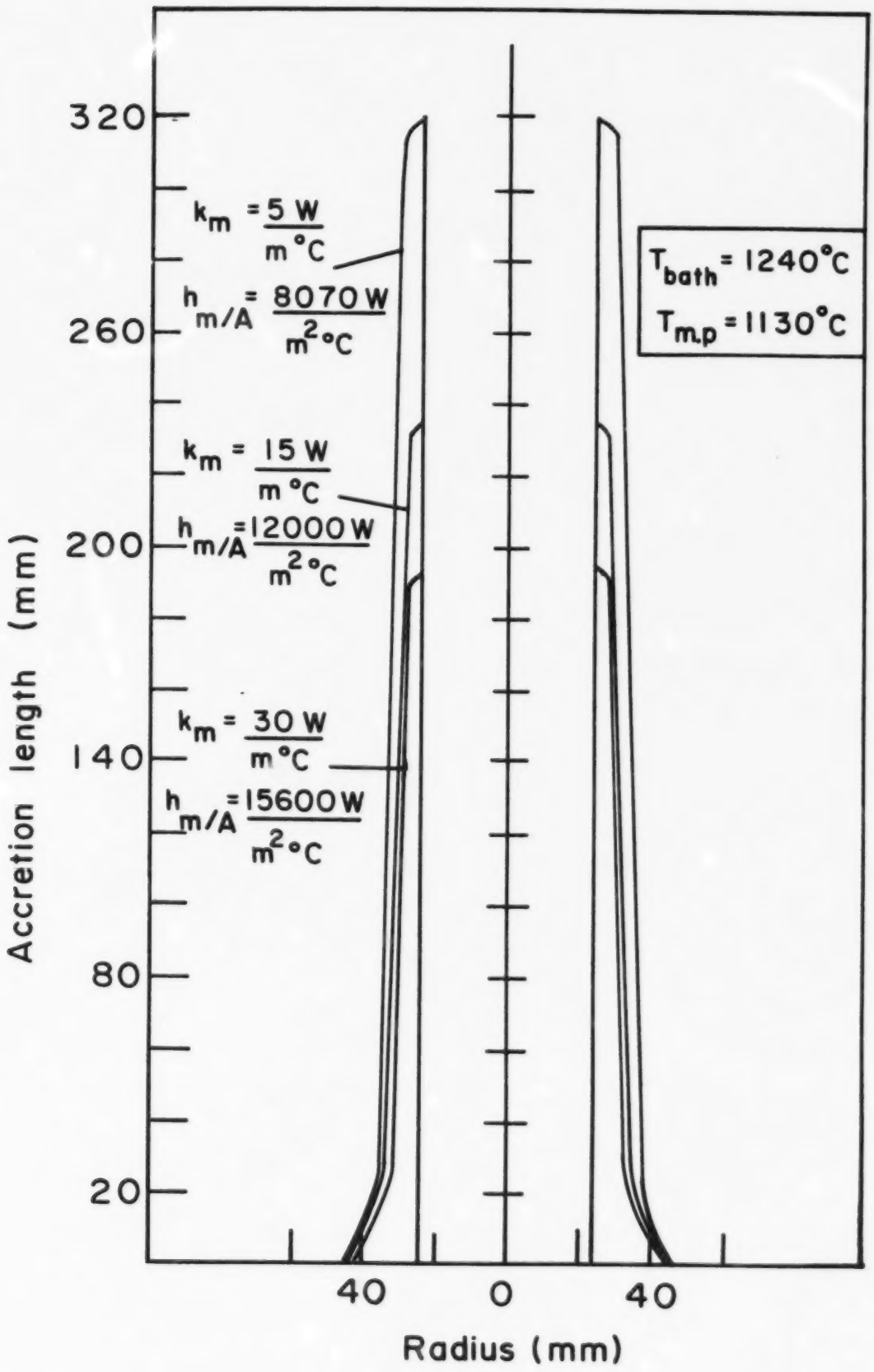

Figure 10. Effect of thermal conductivity of the bath on accretion formation.

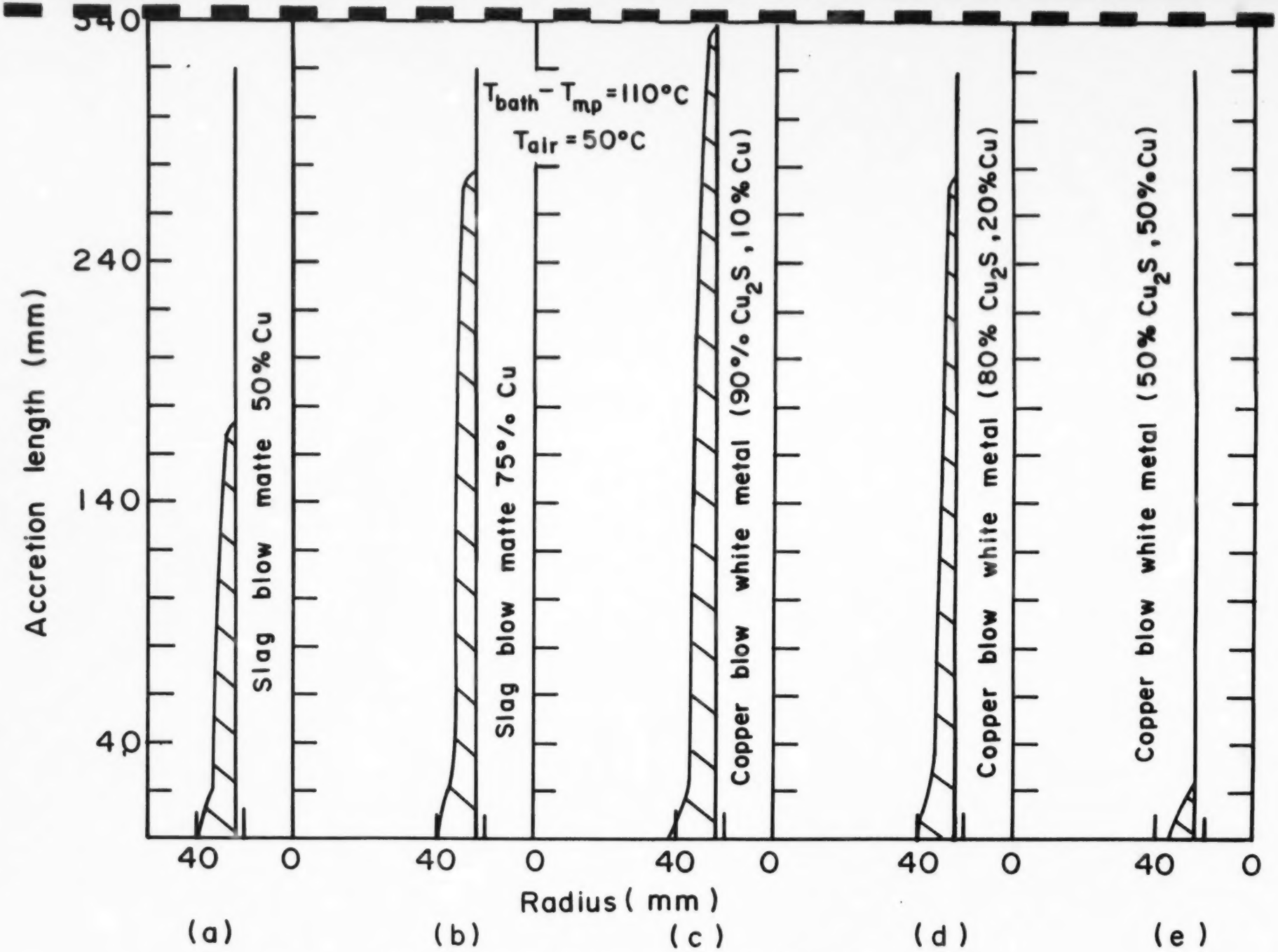

Figure 11. Effect of bath composition on accretion formation.

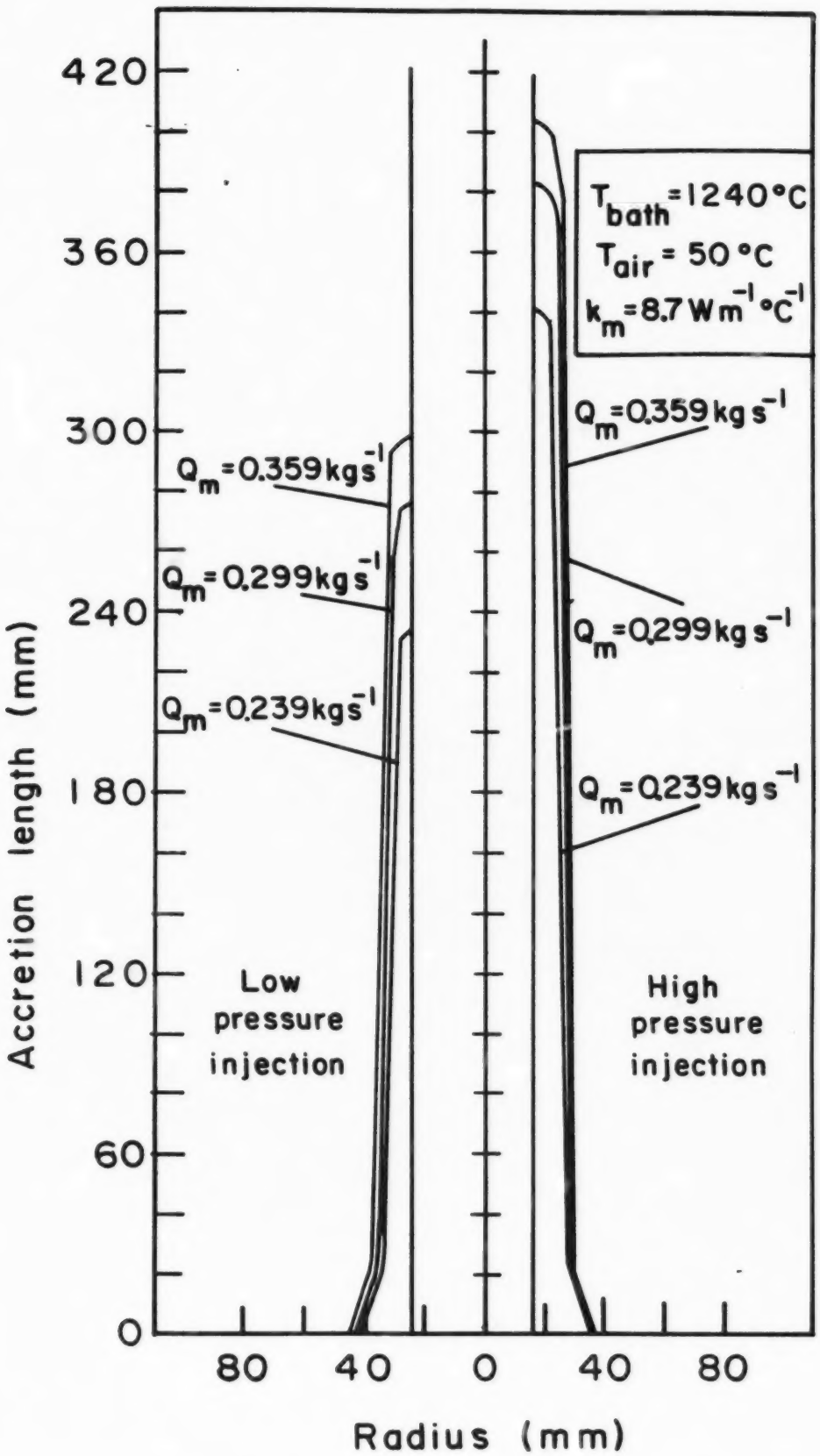

Figure 12. Accretion formation under low-pressure and high-pressure injection conditions.

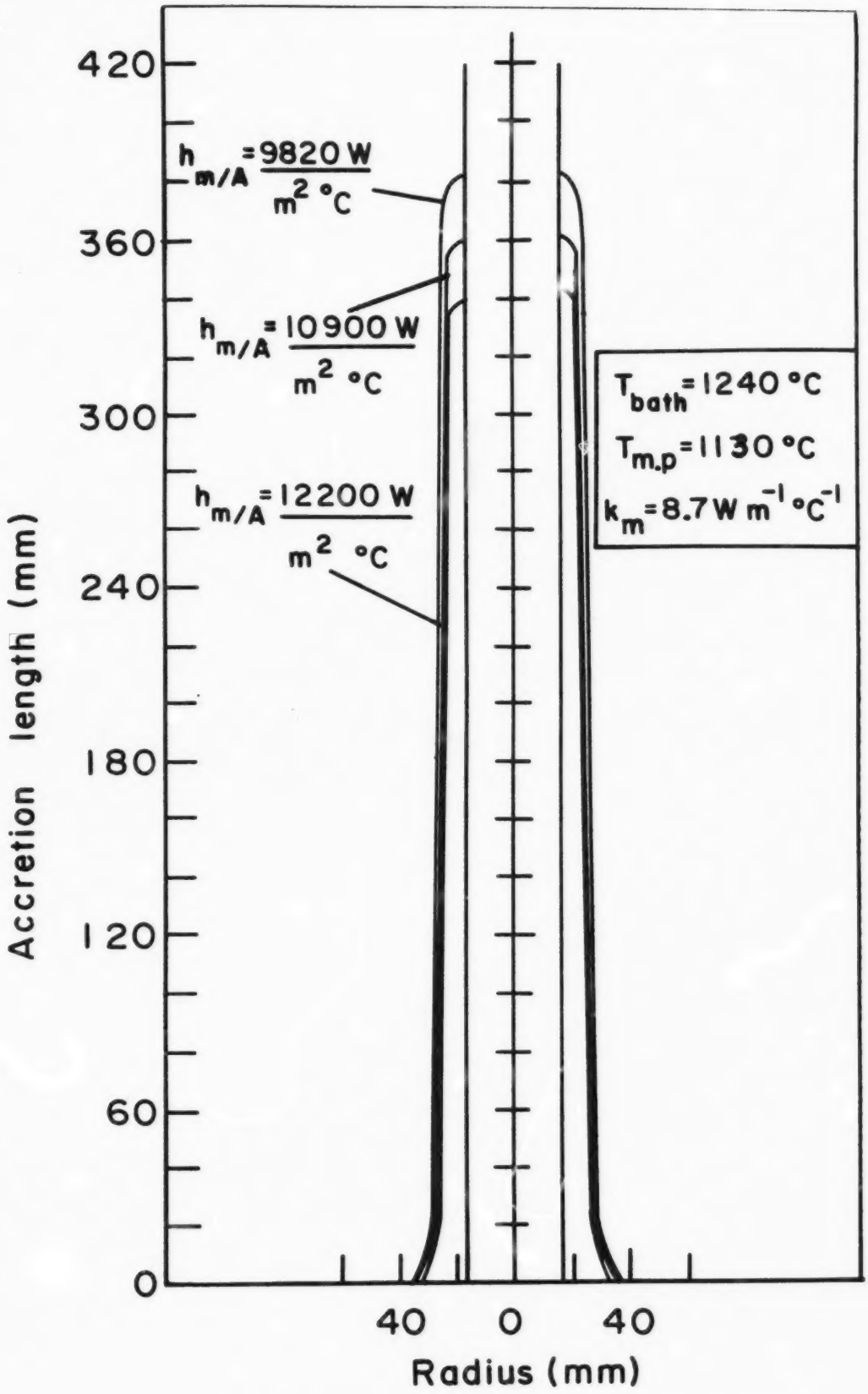

Figure 13. Effect of bath/accretion heat-transfer coefficient under high-pressure injection conditions.

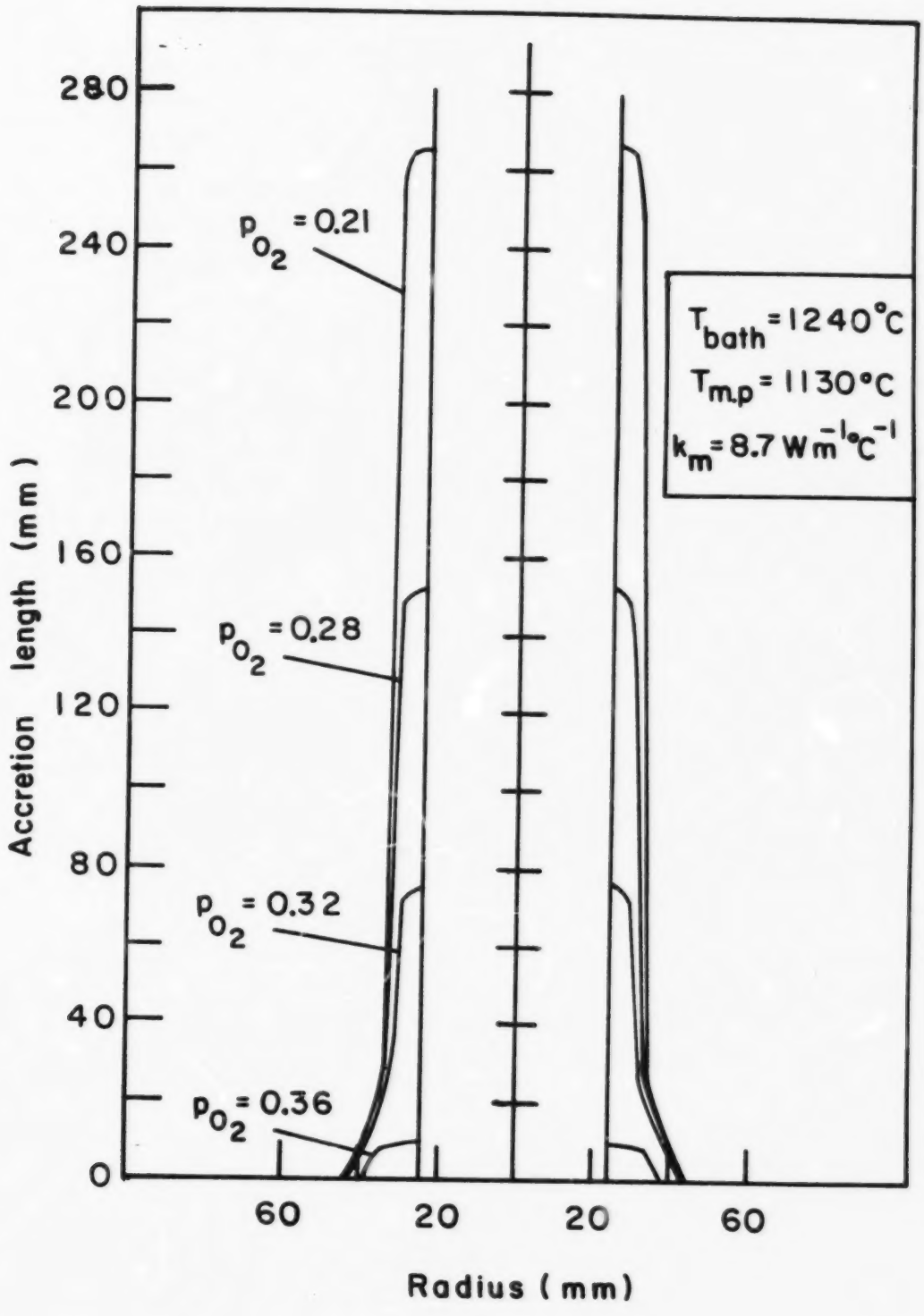

Figure 14. Effect of oxygen enrichment on accretion growth. Low-pressure injection.

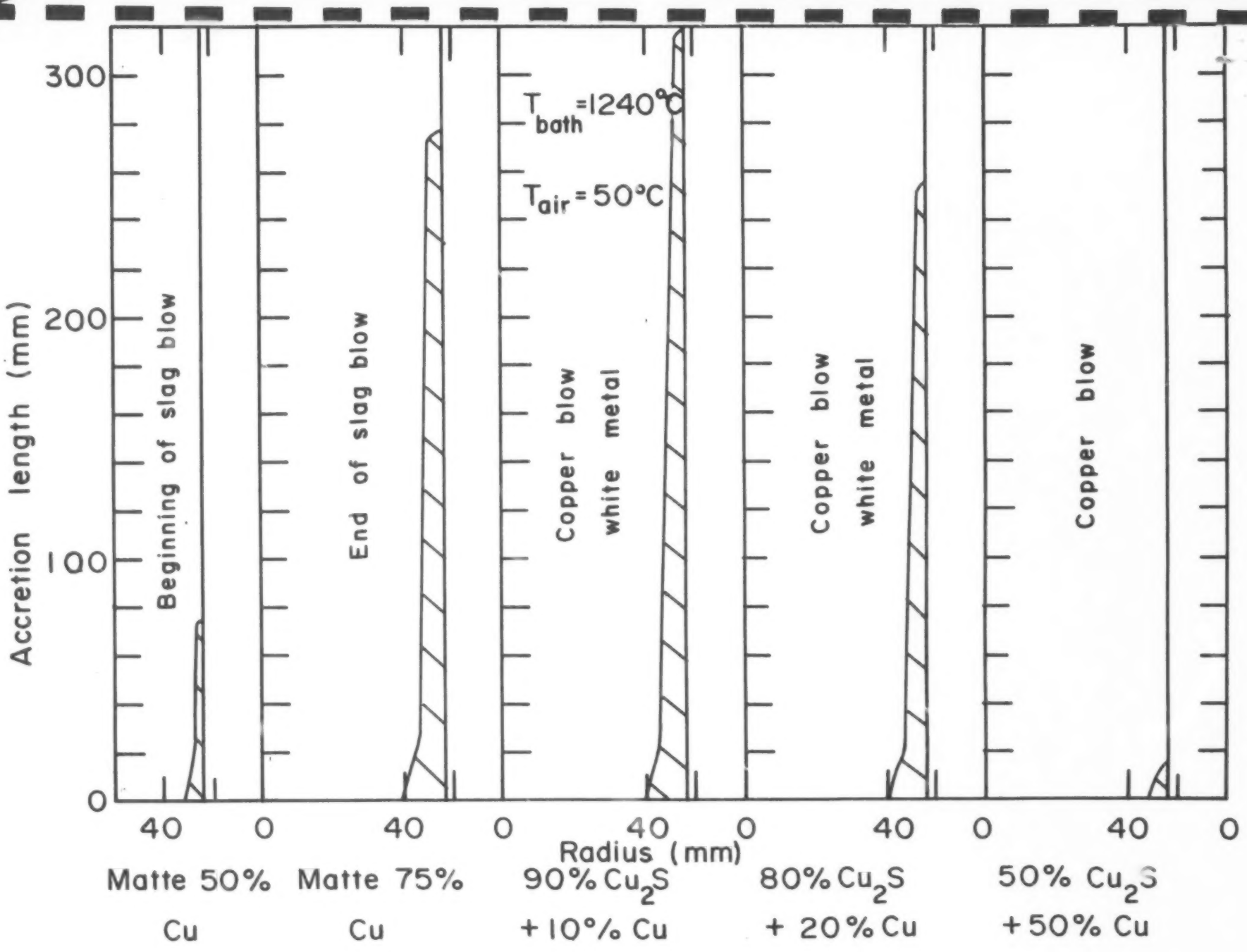

Figure 15. Effect of stage of the blow on accretion formation.